IL-10 Is a Negative Regulatory Factor of CAWS-Vasculitis in CBA/J Mice as Assessed by Comparison with Bruton's Tyrosine Kinase-Deficient CBA/N Mice[1]

Noriko N. Miura,* Motohiko Komai,* Yoshiyuki Adachi,* Naoki Osada,† Yosuke Kameoka,† Kazuo Suzuki,§‡ and Naohito Ohno[2]*

***Candida albicans* water-soluble fraction (CAWS), a mannoprotein-β-glucan complex obtained from the culture supernatant of *C. albicans* NBRC1385, exhibits vasculitis-inducing activity (CAWS-vasculitis) in mice. The sensitivity to CAWS-vasculitis varies greatly among mouse strains. This study examined the factors contributing to or inhibiting CAWS-vasculitis using CAWS-vasculitis-resistant CBA/J mice and Bruton's tyrosine kinase-deficient CBA/N mice, which is a CAWS-vasculitis-sensitive strain that has the same origin as CBA/J mice. After stimulation with various kinds of pathogen-associated molecular patterns, the production of inflammatory cytokines IL-6 and IFN-γ was induced in CBA/N mice, whereas that of immunosuppressive IL-10 was induced in CAWS-vasculitis-resistant CBA/J mice. Furthermore, the production of tissue inhibitor of metalloproteinase 1, an endogenous matrix metalloproteinase inhibitor, was observed in CBA/J mice. The results strongly suggest that the difference in the production of these cytokines is closely linked to the development of CAWS-vasculitis. *The Journal of Immunology*, 2009, 183: 3417–3424.**

Vasculitis syndrome is a collective term for diseases caused by vasculitis, which is defined as inflammation of the vascular wall (endothelium, tunica media, and adventitia) and its adjacent parts. In arteries and veins, vasculitis is characterized by the localized infiltration of inflammatory cells into the intravascular wall and its surroundings, accompanied by denaturation and necrosis. Many diseases, including Takayasu's disease, Wegener's granulomatosis, and Buerger's disease, are known to cause vasculitis. However, the cause of various clinical pathologies or groups of disorders brought about by vasculitis remains unknown. The techniques of molecular biology and genetic engineering are well established, and new technologies have been developed frequently in these fields. Using such technologies, the etiology and pathology of vasculitis is being clarified gradually.

Kawasaki disease was first reported by Dr. T. Kawasaki in 1967 and is also called acute febrile mucocutaneous lymph node syndrome (1). It is a disease characterized by fever continuing for 5 days or longer, hyperemia of bulbar conjunctiva in both eyes, strawberry tongue, and atypical rash; the cause of which is unknown. Systemic vasculitis develops in Kawasaki disease patients. In particular, vasculitis of the coronary artery as sequela is of concern (2). The coronary vasculitis develops further into coronary aneurysm. If the aneurysm is relatively small, it can be normalized within 1 or 2 years in most cases. However, a large aneurysm may result in occlusion by forming a thrombus, complicated with myocardial ischemia and myocardial disorders, and lead to sudden death because of myocardial infarction. In regard to this occasionally lethal vasculitis, although the incidence of coronary disorders has been on the decline because of recently introduced gammaglobulin therapy, neither the pathogenic mechanism nor therapeutic pharmacological mechanism is known (3, 4).

Murata and colleagues et al. (5–7) revealed that arteritis similar to coronary vasculitis, which is known as a sequela of Kawasaki disease, can be induced in mice by *Candida albicans*-derived substances in the forms of a KOH extract of *C. albicans* cell wall. Subsequently, *C. albicans* water-soluble fraction (CAWS)[3] was studied for its ability to induce vasculitis, and it was found to induce vasculitis at a higher rate than *C. albicans*-derived substances. The results indicated that CAWS is very useful for the analysis of the pathogenesis of this disease (8–15).

A deficiency of Bruton's tyrosine kinase (Btk) in humans causes serious sequela. This condition is known as X-linked agammaglobulinemia. Patients with X-linked agammaglobulinemia are vulnerable to infection, and administration of Ig is indicated (16). In mouse, the lack of Btk is called Xid (*xid*), and CBA/N mice have this genetic background (17).

CBA/J and CBA/N mice were differentiated from CBA/H mice, which were derived from DBA mice. In CBA/N mice, several phenomena caused by the lack of Btk have been reported. Btk is believed to be essential for B cell differentiation and maturation. In

*Laboratory for Immunopharmacology of Microbial Products, Tokyo University of Pharmacy and Life Sciences, Tokyo, Japan; †Laboratory of Genetic Resources, National Institute of Biomedical Innovation, Osaka, Japan; ‡National Institute of Infectious Diseases, Tokyo, Japan; and §Graduate School of Medicine and School of Medicine, Chiba University, Chiba, Japan

Received for publication August 6, 2008. Accepted for publication July 4, 2009.

The costs of publication of this article were defrayed in part by the payment of page charges. This article must therefore be hereby marked *advertisement* in accordance with 18 U.S.C. Section 1734 solely to indicate this fact.

[1] This work was partly supported by a grant-in-aid for Scientific Research from the Ministry of Education, Culture, Sports, Science, and Technology of Japan and the Promotion and Mutual Aid Corporation for Private Schools (Japan). This study was also supported by the Ministry of Health, Labour, and Welfare of Japan by a Grant for "Research on Regulatory Science of Pharmaceuticals and Medical Devices" and by the Program for Promotion of Basic and Applied Researches for Innovations in Bio-oriented Industry.

[2] Address correspondence and reprint requests to Dr. Naohito Ohno, Laboratory for Immunopharmacology of Microbial Products, Tokyo University of Pharmacy and Life Sciences, 1432-1 Horinouchi, Hachioji, Tokyo 192-0392, Japan. E-mail address: ohnonao@ps.toyaku.ac.jp

[3] Abbreviations used in this paper: CAWS, *Candida albicans* water-soluble fraction; Btk, Bruton's tyrosine kinase; EVG, Elastica-van-Gieson; MMP, matrix metalloprotease; PAF, platelet-activating factor; PAMP, pathogen-associated molecular pattern; TIMP1, tissue inhibitor of metalloproteinase 1.

www.jimmunol.org/cgi/doi/10.4049/jimmunol.0802484

particular, this enzyme is reported to participate in rearrangement of the L chain gene during pre-B cell differentiation into immature B cells. Consequently, few mature B cells exist in CBA/N mice, and their Ab-producing ability is decreased (18–20). Other effects of the lack of Btk include a decrease in NO production in macrophages, an increase in IL-12 production, and a decrease in IL-5 production from T cells (21, 22).

This study examined the ability of CAWS to induce vasculitis in CBA/N mice, histologically analyzed CBA/N and CAWS-vasculitis-resistant CBA/J mice, and compared the difference in cytokine responses and the inflammatory parameters between CBA/N and CAWS-vasculitis-resistant CBA/J mice. CAWS-vasculitis inhibitory factors were also analyzed.

Materials and Methods

Experimental animals

Male CBA/N and DBA/2 mice were acquired from Japan SLC. Male CBA/J mice were acquired from Charles River Japan. The animals were raised in a specific pathogen-free environment. Mice aged 5–14 wk were used in this study. All animal experiments in Tokyo University of Pharmacy and Life Sciences (TUPLS), and each of the experimental protocols was approved by the Committee of Laboratory Animal Experiments of TUPLS.

Fungi

C. albicans strain NBRC1385 was acquired from the National Institute of Technology and Evaluation Biological Resource Center, stored on Sabouraud agar medium (Difco) at 25°C, and subcultured once every 3 mo.

Preparation of CAWS

CAWS was prepared from *C. albicans* strain NBRC1385 in accordance with conventional methods. Culture was performed in 5 liters of C-limiting medium for 2 days at a rotating speed of 400 rpm while pumping in air at 27°C and 5 L/min. After culturing, an equal volume of ethanol was added, and after allowing to stand undisturbed overnight, the precipitate was recovered. This fraction was dissolved in 250 ml of distilled water, ethanol was added, and the solubilized fraction was allowed to stand undisturbed overnight. The precipitate was recovered and dried with acetone to obtain CAWS.

Administration schedule for induction of CAWS-vasculitis

CAWS (0 or 4 mg/mouse) was administered i.p. for 5 consecutive days to each mouse. At 28 days after CAWS injection, mice were sacrificed, and the hearts of the animals were fixed with 10% neutral formalin and prepared in paraffin blocks. Tissue sections were stained with H&E stain or Elastica-van-Gieson (EVG) stain.

Examination of IL-10 and endogenous matrix metalloproteinase (MMP) inhibitor (tissue inhibitor of metalloproteinase 1 (TIMP1)) mRNA expression levels in aorta by RT-PCR

The spleen and the aorta were resected from mice, frozen in liquid nitrogen, and immediately stored in Isogen (Nippon Gene). Each sample was homogenized with a homogenizer, and RNA was isolated by chloroform extraction. The total RNA level was determined by measuring OD using Nanodrop-ND1000. All total RNA were stored at −80°C or below.

Nuclease-free water was added to the total RNA along with oligo dT_{20} primer (Promega), and the reaction was conducted in a Thermal Cycler (Takara) at 70°C for 5 min. The product was cooled immediately by placing the reaction on ice for 5 min. Then, the following reagents were added: Moloney murine leukemia virus reverse transcriptase XL (Promega), PCR nucleotide mix (dNTP) (Promega), Moloney murine leukemia virus reverse transcriptase 5× reaction buffer, and nuclease-free water. The reverse transcriptase reaction was performed at 42°C for 60 min in a total volume of 25 μl/tube to obtain cDNA. The obtained cDNA was used as a template by adding PCR Master Mix (2×) (Promega), forward primer, reverse primer, and nuclease-free water, and heat denaturation was performed at 94°C for 2 min. One cycle consisted of heat denaturation at 94°C for 10 s, primer annealing at 55°C for 30 s, and elongation at 72°C for 1 min. Thirty cycles of this reaction were performed to obtain the PCR products. The primer sequences are shown as follows, all of which were purchased from Sigma-Genosys: IL-10 forward primer, 5′-ACCTGGTAGAAGTGTATGCCCCAGGCA-3′; IL-10 reverse primer, 5′-CTATGCAGTTGATGAAGATGTCAAA-3′; TIMP1 forward primer, 5′-ACTCGGACCTGGTCATAAGGGC-3′; TIMP1 reverse primer, 5′-AAGAAGCTGCAGGCACTGAT-3′; β-actin forward primer, 5′-TGGAATCCTGTGGCATCCTGAAAC-3′; and β-actin reverse primer, 5′-TAAAACGCAGCTCAGTAACAGTCCG-3′.

Comprehensive analysis of expressed gene by gene chip

We pooled total RNA from the spleens of three DBA/2 and two CBA/J mice for each strain after 21 days from the injection of CAWS. The probes labeled by cyanin3 and cyanin5 were hybridized with a DNA microarray (mouse 10K oligo chip; DNA Chip Consortium) on which 10,386 clones were spotted. After washing, fluorescence was measured using an array scanner. The fluorescence intensity of each spot was corrected by subtracting the background fluorescence intensity. Genes of signal intensity values <1000 were excluded because these may be detected nonspecifically. The microarray data was deposited to Gene Expression Omnibus (accession no. GSE16529; ⟨www.ncbi.nlm.nih.gov/geo/query/acc.cgi⟩).

Spleen cell culture

The mice were euthanized by inhalation of CO_2, after which the spleen was excised. After teasing using a mesh in RPMI 1640 medium, the tissue was separated by centrifugation at 1200 rpm by 5 min, and the resulting cells were treated with Ammonium Chloride Potassium lysing buffer (8.20 g/L NH_4Cl, 1 g/L $KHCO_3$, and 37.2 mg/L EDTA 2Na). After two washes with RPMI 1640 medium, the spleen cells were counted to adjust the cell density and then used after being suspended in RPMI 1640 medium with 10% FCS. The spleen cells were adjusted to 5×10^5 in RPMI 1640 medium containing 10% FCS, and 500-μl aliquots were added to each well of a 48-well plate. After the addition of LPS (from *Escherichia coli* serotype 0111:B4; SIGMA), CpG (1668; 5′-TCCATGACGTTCCTGATGCT-3′; Sigma-Genosys), or tri-acylated lipoproteine (Pam_3-CSK_4), the cells were cultured for 48 h in a 5% CO_2 incubator at 37°C. The cytokine level of the culture supernatant was determined by ELISA as described below.

Measurement of IL-10 and TIMP1

IL-10 level was measured using a OPT_{EIA} IL-10 ELISA kit (BD Pharmingen), and the TIMP1 level was measured using a RayBio Mouse TIMP1 ELISA kit.

Measurement of IFN-γ

A 96-well ELISA plate (Nunc) was coated with rat anti-mouse IFN-γ mAb (BD Pharmingen) using 0.1 M $NaHCO_3$ (pH 8.2) and incubated overnight at 4°C. After washing with 0.05% Tween PBS (PBST), the Ab was blocked for 40 min at 37°C with 0.5% BSA-PBST (BPBST). This was followed by the addition of standards and samples (50 μl each), incubation for 40 min at 37°C, and six washes with PBST. Fifty microliters of a secondary Ab in the form of biotinylated rat anti-mouse IFN-γ (1/1000; BD Pharmingen) was then added, and after incubation for 40 min at 37°C and a wash with PBST, peroxidase-conjugated streptavidin (1/2000; BD Pharmingen) was added. This was followed by incubation for 40 min at 37°C and six washes with PBST. Subsequently, color was generated using peroxidase substrate (tetramethylbenzidine microwell peroxidase substrate system; Kirkegaard & Perry Laboratories). After termination of the reaction with 1 M phosphoric acid, absorbance (OD450/reference OD630) was measured. Recombinant mouse IFN-γ (BD Pharmingen) was used as the standard.

Measurement of IL-6

A 96-well ELISA plate (Nunc) was coated with rat anti-mouse IL-6 mAb (BD Pharmingen) using 0.1 M bicarbonate buffer (pH 9.5) and incubated overnight at 4°C. After washing with PBST, the Ab was blocked for 40 min at 37°C with BPBST. This was followed by the addition of standards and samples (50 μl each), incubation for 40 min at 37°C, and six washes with PBST. Fifty microliters of a secondary Ab in the form of biotinylated rat anti-mouse IL-6 (1/2000; BD Pharmingen) was then added, and after incubation for 40 min at 37°C and a wash with PBST, peroxidase-conjugated streptavidin (1/10,000; BD Pharmingen) was added. This was followed by incubation for 40 min at 37°C and six washes with PBST. Subsequently, 50 μl of peroxidase substrate (tetramethylbenzidine microwell peroxidase substrate system; Kirkegaard & Perry Laboratories) was added to generated color, and absorbance was measured as described previously. Recombinant mouse IL-6 (BD Pharmingen) was used as the standard.

Test for significant difference

Tests for significant differences in this study were performed using Student's *t* test, and values with $p < 0.05$ were judged significant.

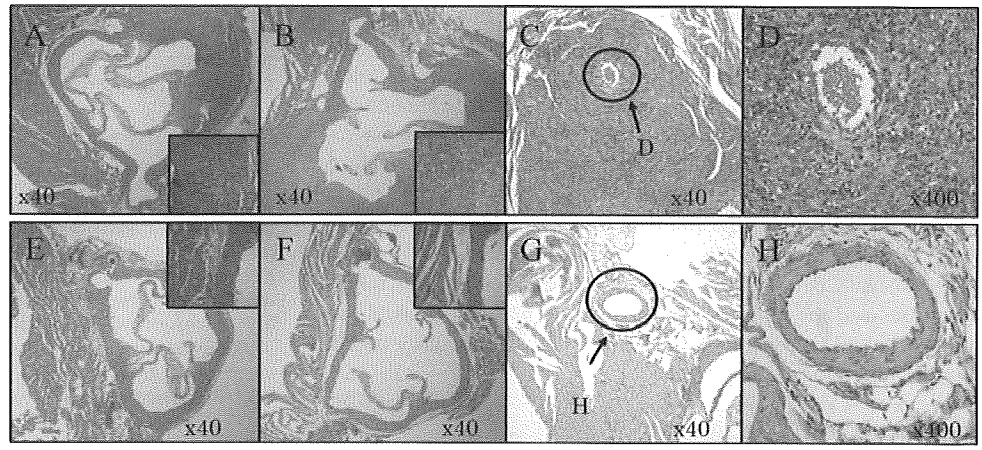

FIGURE 1. Histopathological findings of coronary arteries and aorta in CBA/N and CBA/J mice. CAWS (4 mg/mouse) was i.p. administered to CBA/N (*A–D*) and CBA/J (*E–H*) mice for 5 consecutive days. At 14 (*A* and *E*) and 28 (*B–D* and *F–H*) days after CAWS injections, mice were sacrificed and stained using H&E.

Results

Histological analysis of CAWS-vasculitis in CBA/J and CBA/N mice

Following the protocol for CAWS-vasculitis induction, CAWS was administered to CBA/J and CBA/N mice, and tissue slices of the beginning of aorta were prepared and stained with HE and EVG for observation. As a result, a 100% incidence of vasculitis was observed in the aorta and coronary artery of CBA/N mice (Fig. 1, *A–D*). This vasculitis in CBA/N mice developed 2 wk after the administration of CAWS. In contrast, no significant inflammatory changes were observed in the intima or adventitia of the aorta or the coronary artery in CBA/J mice (Fig. 1, *E–H*). EVG staining revealed injuries to the elastic fibers of CBA/N mice, which developed into CAWS-vasculitis, but similar injuries were not observed in CAWS-vasculitis-resistant CBA/J mice (Fig. 2).

cDNA microarray analysis of gene expression in spleen

To determine factors that participated in the onset of CAWS-vasculitis, genome-wide patterns of gene expression in challenged mice were examined using DNA microarrays. DBA/2 was only the strain in the present experiments that died because of CAWS-vasculitis. On the other hand, CBA/J mice showed the strongest resistance to CAWS-vasculitis among the inbred strains used in these experiments. To compare the difference in gene expression in the spleen at the time of vasculitis development between DBA/2 and CBA/J mice, a comprehensive analysis of the difference among strains was performed using the oligo-DNA microarrays.

As genes showing low expression in the hybridization detection system are not reliable, spots with a sum of cyanin3 and cyanin5 fluorescence intensities exceeding 1000 and having differences of $\geq$1.5 times were selected. According to these criteria, 271 genes were up-regulated in CBA/J mice, and 148 genes were up-regulated in DBA/2 mice. Genes with unknown function in the public database were filtered out. A list of differentially expressed genes was shown in Table I. In DBA/2 mice, the expression of inflammatory genes, such as *cathepsin G*, *myeloperoxidase*, *proteinase 3*, and *neutrophil elastase*, was increased, whereas in CBA/J mice, that of *TIMP1* was increased.

As described above, DBA/2 mice are the most sensitive strain to CAWS-vasculitis, and CBA/J is the most resistant. Many inflammatory as well as anti-inflammatory genes were differentially expressed between CBA/J and DBA/2 strains, suggesting that genes responsible for inflammation may play an important role for vasculitis. In this study, a third strain, CBA/N, which exhibits Btk deficiency and it is moderately sensitive to CAWS-vasculitis, was used, as shown in Figs. 1 and 2. At present, it was decided not to carry out microarray analysis using CBA/N because of its intermediate phenotype. However, this strain is superior for quantitative experiments, as shown later (Fig. 3).

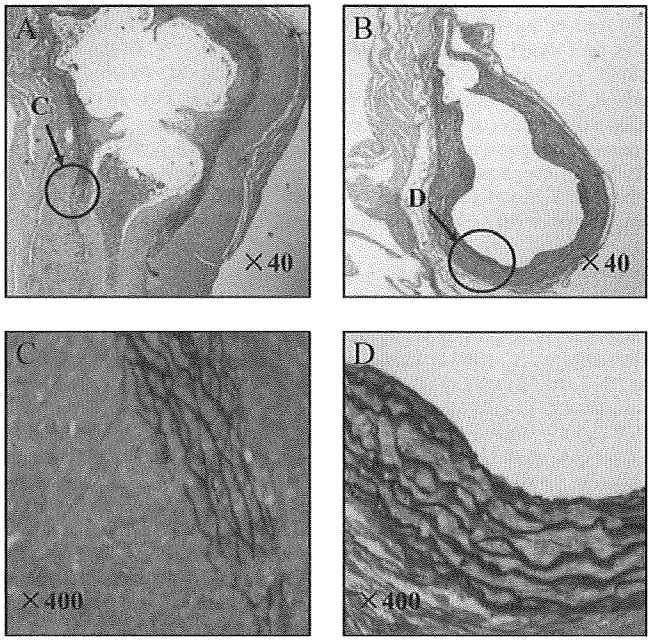

FIGURE 2. Histopathological findings of coronary arteries and aorta. CAWS (4 mg/mouse) was i.p. administered to CBA/N (*A* and *C*) and CBA/J (*B* and *D*) mice for 5 consecutive days. At 28 days after CAWS injections, mice were sacrificed and stained with EVG stain.

Blood cytokine production in the initial phase after CAWS administration

CBA/J is the only mouse strain resistant to CAWS-vasculitis among the inbred mouse strains studied so far. It was reported previously that anti-inflammatory cytokine IL-10 (23) production is increased in CBA/J mice (11). Therefore, the serum IL-10 level was measured in CBA/J and CBA/N mice after administration of CAWS (4 mg in PBS/mouse), along with the production of TIMP1, an endogenous matrix metalloprotease inhibitor, the gene expression level of which was found to be increased in the cDNA microarray analysis.

In CBA/J mice, high levels of IL-10 were produced 1 h after CAWS administration. In contrast, IL-10 production was hardly detected in CBA/N mice (Fig. 3*A*). In CBA/J mice, TIMP1 showed high levels 4 h after CAWS administration, and it continued to increase even at 10 h after CAWS administration. On the other

Table I. *Genes differentially expressed in CBA/J and DBA/2 splenocytes at day 21*[a]

Gene Name	Log_2 Ratio	UniGene
Myeloperoxidase	3.04	Mm.4668
Neutrophilic granule protein	2.79	Mm.2827
TNF (ligand) superfamily, member 12	2.73	Mm.8983
S100 calcium-binding protein A9 (calgranulin B)	2.58	Mm.2128
Cathelicidin antimicrobial peptide	2.50	Mm.21855
Peptideglycan recognition protein	2.47	Mm.3834
Cathepsin G	2.30	Mm.4858
S100 calcium-binding protein A8 (calgranulin A)	2.27	Mm.21567
GATA-binding protein 1	2.05	Mm.1344
CD24a Ag	2.02	Mm.6417
Hemoglobin Z, β-like enbrionic chain	1.90	Mm.196718
Lipocalin 2	1.89	Mm.9537
Carbonic anhydrase 1	1.82	Mm.3471
Chemokine (C-X-C motif) ligand 7	1.62	Mm.157750
Fibronectin 1	1.51	Mm.193099
Chemokine (C-X-C motif)ligand 4	1.50	Mm.23905
Neutrophil elastase	1.39	Mm.271137
Proteinase 3	1.35	Mm.2364
Aminolevulinate, δ-,dehydratase	1.34	Mm.6988
TNF, α-induced protein 2	1.28	Mm.4348
Chemokine (C-X-C motif) receptor 4	1.18	Mm.1401
C-type lectin-like receptor 2	1.12	Mm.30700
IFN-stimulated protein	1.11	Mm.19029
Chemokine(C-X-C motif) ligand 5	0.99	Mm.4660
Chemokine (C-C motif) receptor 1-like 1	0.95	Mm.57056
IL-12R, β1	0.95	Mm.731
TGF-β1-induced transcript 4	0.94	Mm.20927
TIMP1	−5.44	Mm.8245
Insulin 1	−5.20	Mm.46269
Chemokine (C-C motif) receptor 8	−4.89	Mm.8000
IL-8R, β	−4.43	Mm.234466
Carboxyl ester lipase	−4.43	Mm.4349
Carboxypeptidase B1 (tissue)	−4.30	Mm.34692
Regenerating islet-derived 2	−4.25	Mm.46360
Pancreatic lipase-related protein 2	−4.14	Mm.1230
Glycoprotein hormones, α subunit	−4.10	Mm.1361
Serine protease inhibitor, Kazal type 3	−4.04	Mm.272
Elastase 1, pancreatic	−3.97	Mm.2131
Regenerating islet-derived 1	−3.97	Mm.142731
Protease, serine, 18	−3.94	Mm.3944
Pancreatic lipase-related protein 1	−3.66	Mm.10753
Chemokine(C-X-C motif) ligand 11	−3.33	Mm.131723
Cholinergic receptor, nicotinic, β-polypeptide 1	−2.97	Mm.86425
Elastase 2	−2.92	Mm.21925
Pancreatitis-associated protein	−2.71	Mm.2553
Chymotrypsin-like	−2.70	Mm.2745
Inhibitor of κB kinase γ	−2.60	Mm.12967
Islet neogenesis-associated protein-related protein	−2.53	Mm.33691
Protease, serine, 21	−2.35	Mm.86657
TNFR superfamily, member 12a	−1.85	Mm.28518
Inter-α trypsin inhibitor, heavy chain 1	−1.75	Mm.3227
Carboxipeptidase A1	−1.64	Mm.25377
Thioredoxin 1	−1.31	Mm.260618

[a] The genes with negative ratio values are abundant in the CBA/J mice, whereas genes with positive ratio values are abundant in the DBA/2. The microarray data was deposited to Gene Expression Omnibus (accession no. GSE16529; www.ncbi.nlm.nih.gov/geo/query/acc.cgi).

hand, in CBA/N mice, TIMP1 showed high levels 4 h after CAWS administration similar to CBA/J mice, but it decreased at 10 h after CAWS administration (Fig. 3*B*).

Gene expression levels in the spleen and the aorta in the initial phase after CAWS administration

The gene expression levels of anti-inflammatory cytokines were compared in the initial phase after CAWS administration in CBA/J and CBA/N mice. CAWS (4 mg/0.2 ml PBS) was administered i.p., and the effect was examined using RT-PCR to measure IL-10 and TIMP1 gene expression levels in the spleen and the aorta 1 and 3 h after the administration (Fig. 4). β-Actin was used as the internal standard and for correcting the expression level of each sample.

IL-10 gene expression in spleen cells at 1 and 3 h after CAWS administration was higher in CBA/J mice than in CBA/N mice. In particular, high expression levels were observed 1 h after CAWS

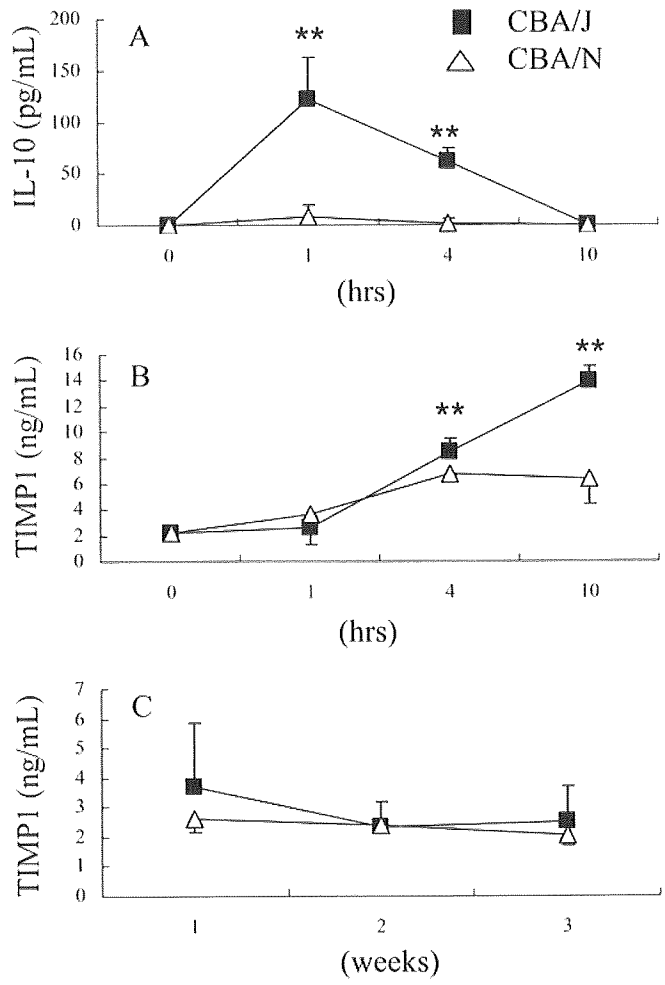

FIGURE 3. Serum IL-10 and TIMP1 leads to CAWS-injected CBA/J and CBA/N mice. Serum was collected from CBA/J and CBA/N mice i.p. injected with CAWS (4 mg/mouse) at various time points (six animals per group). IL-10 (*A*) and TIMP1 (*B*; after 0, 1, 4, 10 hours of CAWS administration, *C*; after 1, 2, 3 wk of CAWS administration) production was measured using ELISA. *, $p < 0.05$; **, $p < 0.001$ (vs 0 h).

administration. It was also observed that TIMP1 gene expression was increased in CBA/J mice after CAWS administration. However, contrary to the expectation, a particularly high expression was observed in CBA/N mice 3 h after CAWS administration (Fig. 4, *A* and *C*).

A markedly higher expression level of IL-10 gene in aorta cells of CBA/J mice was noted 1 h after CAWS administration. The IL-10 gene expression level in CBA/N mice was lower than that in CBA/J mice, but the TIMP1 gene expression level was similar in both strains before and after the administration of CAWS (Fig. 4, *B* and *D*).

Blood cytokine production in the late phase after CAWS administration

It was reported that CAWS-vasculitis begins to develop ~1 wk after CAWS administration (10). Using ELISA, serum cytokine production was measured in the late phase after CAWS administration (4 mg/0.2 ml PBS) when the vasculitis was thought to have developed (Fig. 3*C*).

IL-10 production was not observed in either CBA/J or CBA/N mice in the late phase after CAWS administration (data not shown). After 1 wk of CAWS administration, TIMP1 production in CBA/J mice tended to be higher but not to a significant degree.

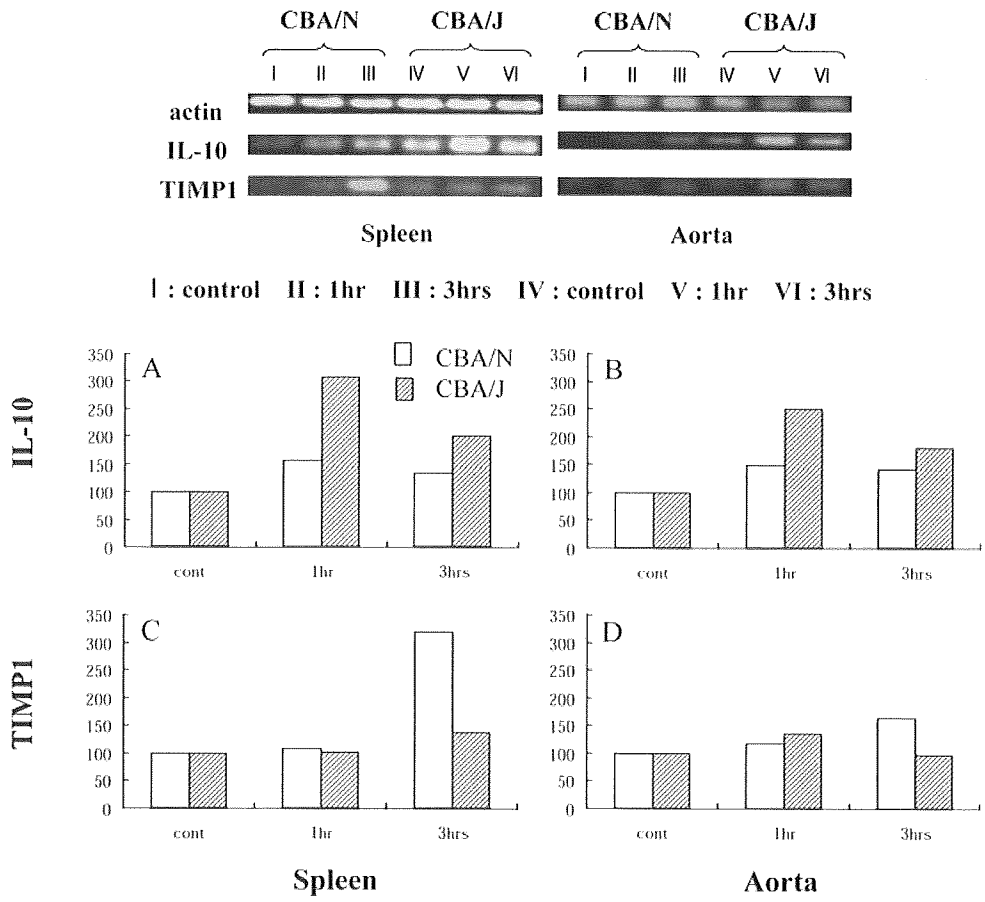

FIGURE 4. Semiquantitative analysis of IL-10 and TIMP1 mRNA expression ratios relative to actin in the spleen and aorta. Total RNA was isolated from the spleen and the aorta of CBA/J and CBA/N mice i.p. injected with CAWS (0 or 4 mg/mouse) at various time points. After the reverse transcriptase reaction was performed, each gene expression level was measured by semiquantitative PCR. Actin mRNA expression was also measured as an internal control and used for the normalized of target genes expression levels. *A*, IL-10 mRNA expression level in the spleen; *B*, IL-10 mRNA expression level in the aorta; *C*, TIMP1 mRNA expression level in the spleen; and *D*, TIMP1 mRNA expression level in the aorta.

TIMP1 production in CBA/J mice was not different from that in CBA/N mice after 2 or 3 wk of CAWS administration.

Gene expression in the spleen and the aorta in late phase after CAWS administration

IL-10 and TIMP1 gene expression levels were compared in the spleen and the aorta of CBA/J and CBA/N mice during the vasculitis-forming phase after CAWS administration. CAWS (4 mg/0.2 ml PBS) was administered i.p. for 5 consecutive days, and IL-10 and TIMP1 gene expression levels were examined by RT-PCR in the spleen and the aorta 2 and 4 wk after the last administration.

High IL-10 gene expression levels were observed in both the spleen and the aorta of CBA/J mice 2 wk after CAWS administration (Fig. 5). On the other hand, no IL-10 gene expression was observed in CBA/N mice. High TIMP1 gene expression was noted in the aorta of CBA/J mice 2 and 4 wk after CAWS administration. In addition, in the late phase after CAWS administration, the gene expression level in the spleen and the aorta showed a similar pattern.

Cytokine production in spleen cells of CBA/J and CBA/N mice after stimulation with pathogen-associated molecular patterns (PAMP)

Previous studies have indicated that when spleen cells of DBA/2 and CBA/J mice in which vasculitis had been induced by CAWS were cultured with CAWS the production of non-anti-inflammatory cytokines but not inflammatory cytokines was observed in DBA/2 mice, whereas the production of non-inflammatory cytokines but not anti-inflammatory cytokine IL-10 was observed in CBA/J mice (11). Therefore, the production of IL-10 and inflammatory cytokines IL-6 and IFN-γ was studied in CBA/J and CBA/N mice. The following PAMP were used: LPS, a Gram-negative bacterial cell wall component recognized by TLR4; PAM3, which is recognized by TLR2; and CpG, a synthetic oligodeoxynucleotide recognized by TLR9.

Upon stimulation with these PAMP recognized by respective TLR, the production of a large amount of IL-10 was observed in the spleen cells of CBA/J mice, which show resistance to CAWS-vasculitis. The production of IL-6 and IFN-γ was hardly observed in the spleen cells of CBA/J mice. On the other hand, in the spleen cells of CBA/N mice, which are sensitive to CAWS-vasculitis, the production of IL-6 and IFN-γ but not IL-10 was observed (Fig. 6).

Acute lethal activity in CAWS-administered mice

Other than its vasculitis-inducing activity, CAWS is known for its acute lethal activity after i.v. administration (12, 13). As a positive control, a closed colony of ICR mice was used, in which ~100% acute lethal activity is observed. A 200-μg acute lethal dose of CAWS was administered to the closed-colony ICR mice, in addition to 400 μg of CAWS, which is double that amount, through the caudal vein of the mice.

The acute lethal activity of CAWS was clearly observed in vasculitis-resistant CBA/J mice. CBA/J mice showed reduced movement ~5 min after CAWS administration and shock status ~15 min after administration. Almost all the mice died within 25 min after administration. In contrast, no acute lethal activity was observed in vasculitis-sensitive CBA/N mice, and acute lethal activity was also not observed in DBA/2 mice that develop severe vasculitis (Table II).

Discussion

Kawasaki disease induces the development of systemic vasculitis. In particular, the vasculitis that develops in the coronary artery

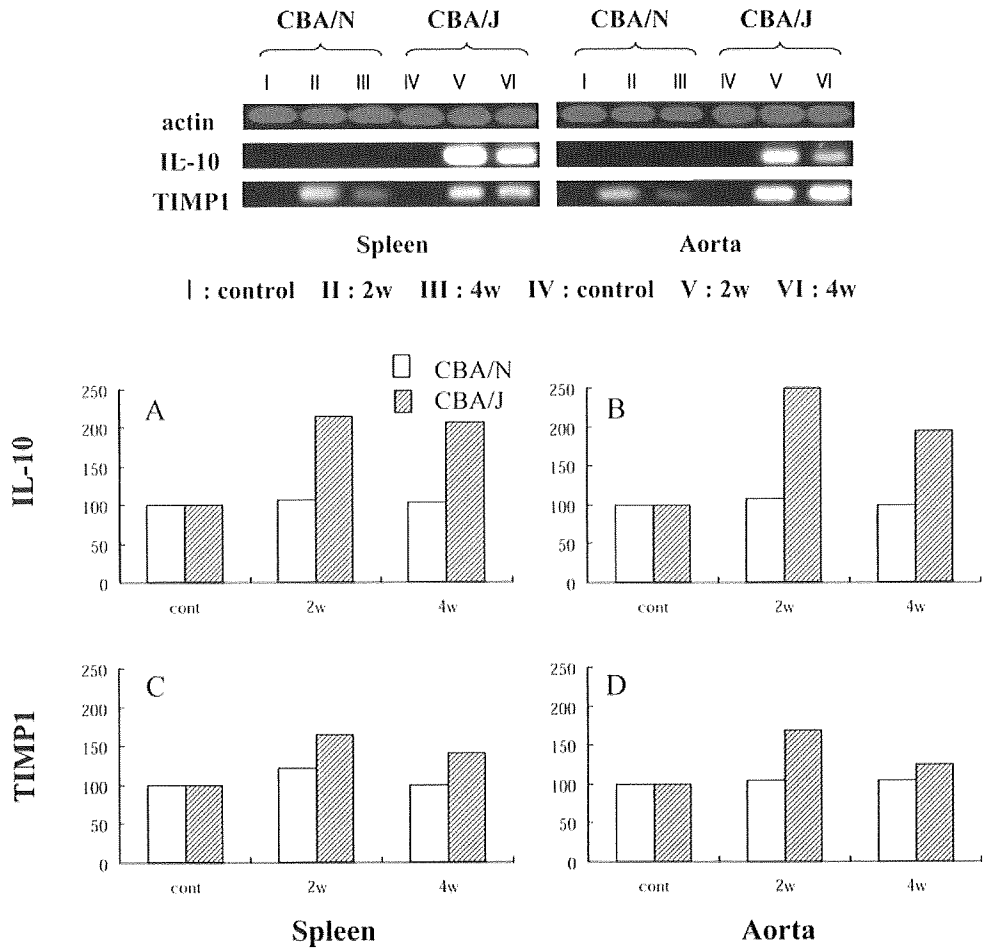

FIGURE 5. Semiquantitative analysis of IL-10 and TIMP1 mRNA expression ratios relative to actin in the spleen and the aorta. Total RNA was isolated from the spleen and the aorta of CBA/J and CBA/N mice i.p. injected with CAWS (0 or 4 mg/mouse) at various time points. After the reverse transcriptase reaction was performed, each gene expression level was measured by semiquantitative PCR. Actin mRNA expression level was also measured as an internal control and used for the normalized of target genes expression levels. *A*, IL-10 mRNA expression level in the spleen; *B*, IL-10 mRNA expression level in the aorta; *C*, TIMP1 mRNA expression level in the spleen; and *D*, TIMP1 mRNA expression level in the aorta.

sometimes becomes lethal, and thus, elucidation of the mechanisms underlying its pathogenesis and therapy is clinically important. According to Murata and colleagues (5–7), when CAWS is i.p. administered daily, vasculitis in the coronary artery, similar to that in Kawasaki disease, can be induced at a high rate. Although the vasculitis-inducing activity of CAWS has been studied in various inbred mouse strains, it was revealed for the first time that CAWS-vasculitis can be induced in Btk-deficient CBA/N mice (Figs. 1 and 2). Analysis of serial sections of the aorta stained with H&E suggested that the vasculitis in CBA/N mice was mild compared with that in DBA/2 mice, because aortic stenosis was mild and no reduction in survival rate was observe after CAWS administration (10, 14). Previous studies have shown that elastic fiber injury occurs in the aorta close to the beginning of the coronary artery in mice that develop CAWS-vasculitis (10). A similar phenomenon was observed in CBA/N mice as well. Because such a phenomenon was not observed in CAWS-vasculitis-resistant CBA/J mice, a rupture of the elastic fibers in CBA/N mice was thought to be attributable to CAWS-vasculitis. The aorta is an elastic-type artery, and this elasticity is due to the formation of a substantial elastic layer in the tunica media. The upper part of the aorta where CAWS-vasculitis occurs is particularly rich in elastic fibers. Therefore, the present observation that injury occurs in the aortic elastic fibers in CBA/N mice as a result of CAWS-vasculitis is an important finding for further analysis of CAWS-vasculitis in the future.

CBA/J mice showed resistance to CAWS-vasculitis. To the best of our knowledge, no inbred mouse strain, except for CBA/J, is resistant to CAWS-vasculitis. Therefore, further analysis of resistance to CAWS-vasculitis in CBA/J mice is considered to be important not only for the elucidation of the pathogenic mechanism of CAWS-vasculitis but also for the development of a therapeutic model. On the other hand, DBA/2 mice develop severe vasculitis following CAWS administration, and this vasculitis is fatal. No other strains of mice, except for DBA/2, showed fatal CAWS-vasculitis. To determine the factors that participated in the onset of CAWS-vasculitis, mRNA expression in the splenocytes from DBA/2 and CBA/J mice was examined using a microarray technique. High expression levels of mRNA such as myeloperoxidase, cathepsin G, neutrophil elastase, and proteinase 3 were recognized in DBA/2 mice. These proteins are well-known markers of neutrophils and correlate with inflammation.

TIMP1 was suggested to be one of the most important factors in the inhibition of CAWS-vasculitis in the results of the microarray analysis (Table I). TIMP1 is known to be a MMP-specific endogenous inhibitor. Contrary to expectation, temporarily high levels of TIMP1 were observed in CBA/J mice (Fig. 3). It was reported that there was no correlation between blood TIMP and MMP production levels and disease severity in multiple patients with Kawasaki disease, and an imbalance of these levels contributed to the development of vasculitis (24, 25). It was also suggested that the imbalance of TIMP and MMP is a factor contributing to the development of vasculitis. MMP was reported to be involved in vasculitis remodeling and the formation of vasculitis in Kawasaki disease (26). Therefore, further studies may be necessary to examine not only TIMP levels per se but also its production level relative to MMP.

The gene expression levels of IL-10 and TIMP1 in spleen and aortic root were examined at early and late stages of CAWS-vasculitis (Figs. 4 and 5). In the late stage (2–4 wk after CAWS

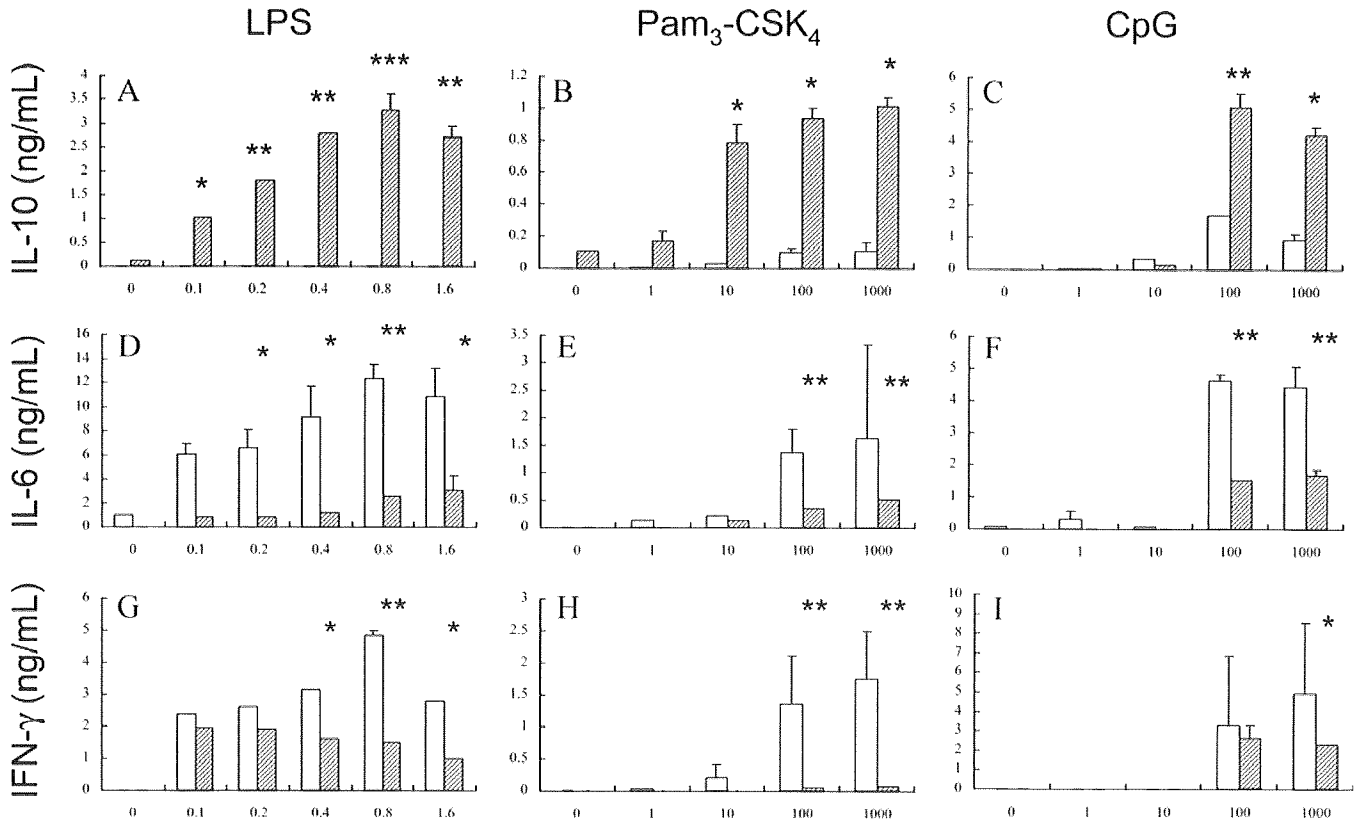

FIGURE 6. Cytokine production in culture supernatants of splenocytes from CBA/J and CBA/N mice stimulated with LPS, PAM_3-CSK_4, and CpG-oligodeoxynucleotide. Splenocytes were collected from CBA/J and CBA/N mice (four animals per group). Prepared splenocytes were cultured with LPS (0, 0.1, 0.2, 0.4, 0.8, or 1.6 μg/ml, *A*, *D*, *G*), PAM_3-CSK_4 (0, 1, 10, 100, or 1000 ng/ml, *B*, *E*, *H*), or CpG-ODN (0, 1, 10, 100, or 1000 nM, *C*, *F*, *I*) for 48 h at an initial density of 5×10^6 cells/ml. The culture supernatants were collected and measured for IL-10 (*A–C*), IL-6 (*D–F*), and IFN-γ (*G–I*) levels using ELISA. □, CBA/N; ▨, CBA/J. *, $p < 0.05$; **, $p < 0.001$ (vs blank).

administration), CAWS-vasculitis had developed, and the infiltration of leukocytes in CBA/N mice was significant. In contrast, leukocyte infiltration into the aortic root was scarce in CBA/J mice (Figs. 1 and 2). It was of interest that both IL-10 and TIMP1 were highly expressed in the aortic root of CBA/J mice. IL-10 acts as anti-inflammatory, and TIMP1 protects tissues from proteases; thus, the expression of both genes concomitantly protects the tissue from inflammation. In the case of CBA/N mice, TIMP1 was expressed weakly, but no IL-10 expression could be detected. The anti-inflammatory system of the aortic root could be weak. Of interest, gene expression in the aortic root and spleen are similar for both genes, suggesting that inflammatory and/or anti-inflammatory states may not be local but systemic. In the early stage of CAWS-vasculitis, when leukocyte infiltration is scarcely induced in both strains of mice, both IL-10 and TIMP1 expression levels were also high in CBA/J mice. From both the results of early and late stages, it was suggested that cells expressing IL-10 and TIMP1 may not be infiltrating inflammatory cells but resident cells of the aortic tissue, such as endothelial cells, fibroblasts, and smooth muscle cells, as well as resident macrophages. However, precise characterization of the cells expressing anti-inflammatory cytokines and molecules was not performed in this study.

Table II. *Acute lethal toxicity of CAWS i.v. administrated mice*[a]

	CBA/J	CBA/N	DBA/2	ICR
200 μg/mouse	4/5	0/5	0/5	5/5
400 μg/mouse	5/5	0/5	0/5	5/5

[a] The acute lethal toxicity of CAWS was monitored after i.v. administration to ICR mice and observing the mice that died within 1 h after administration.

Stimulation of spleen cells of both CBA/J and CBA/N mice with various PAMP revealed high IL-10 production in the spleen cells of CBA/J mice (Fig. 6). It is known that PAMP are mainly recognized by TLR on the cell surface (27). On the other hand, IL-10 was barely produced in the spleen cells of CBA/N mice, whereas the production of inflammatory cytokines IL-6 and IFN-γ was observed. Such cytokine responses are thought to be a factor contributing to the development of CAWS-vasculitis in CBA/N mice. As described earlier, CBA/N mice have a genetic background lacking Btk compared with wild-type CBA/J mice. Therefore, it was strongly suggested that Btk is involved in the difference in IL-10 production between the two mouse strains.

As a result of studies on acute lethal activity after CAWS administration in various inbred mouse strains, in which vasculitis-inducing activity is obvious, this study observed acute lethal activity in vasculitis-resistant CBA/J mice. In contrast, vasculitis-sensitive CBA/N and DBA/2 mice did not show acute lethal activity (Table II). Although the mechanism underlying the development of acute lethal activity has not been completely elucidated, the fact that CAWS is a mannoprotein-β-glucan complex suggests that the complement lectin pathway is involved (28). It was also speculated that in accordance with the activation of the complement lectin pathway by CAWS, anaphylatoxin production and subsequent production of platelet-activating factor (PAF) are activated. PAF is suggested to play an important role in the shock observed when yeast mannan is administered (29). It was reported that PAF receptor induces the production of IL-10 (30–34). However, it remains unknown whether Btk, which is the genetic

difference between CBA/J and CBA/N mice, affects these pathways or not.

From these results, CBA/J mice are thought to be resistant to vasculitis because the inhibitory pathway, including IL-10, is easily induced not only by CAWS but also by various ligands.

Acknowledgments

We thank Hiroki Sankawa for excellent technical assistance.

Disclosures

The authors have no financial conflict of interest.

References

1. Kawasaki, T., and F. Kousaki. 1967. Febrile oculo-oro-cutaneo-acrodesquamatous syndrome with or without acute nonsuppurative cervical lymphadenitis in infancy and childhood: clinical observations of 50 cases (in Japanese). *Jpn. J. Allergy* 16: 178–222.
2. Newburger, J. W., M. Takahashi, M. A. Gerber, M. H. Gewitz, L. Y. Tani, J. C. Burns, S. T. Shulman, A. F. Bolger, P. Ferrieri, R. S. Baltimore, et al. 2004. Diagnosis, treatment, and long-term management of Kawasaki disease: a statement for health professionals from the Committee on Rheumatic Fever, Endocarditis and Kawasaki Disease, Council on Cardiovascular Disease in the Young, American Heart Association. *Circulation* 110: 2747–2771.
3. Newburger, J. W., M. Takahashi, A. S. Beiser, J. C. Burns, J. Bastian, K. J. Chung, S. D. Colan, C. E. Duffy, D. R. Fulton, and M. P. Glode. 1991. A single intravenous infusion of gammaglobulin as compared with four infusions in the treatment of acute Kawasaki syndrome. *N. Engl. J. Med.* 324: 1633–1639.
4. Furusho, K., T. Kamiya, H. Nakano, N. Kiyosawa, K. Shinomiya, T. Hayashidera, T. Tamura, O. Hirose, Y. Manabe, and T. Yokoyama. 1984. High-dose intravenous gammaglobulin for Kawasaki disease. *Lancet* 2: 1055–1058.
5. Murata, H., H. Iijima, S. Naoe, T. Atobe, T. Uchiyama, and S. Arakawa. 1987. The pathogenesis of experimental arteritis induced by *Candida* alkali extract in mice. *Jpn. J. Exp. Med.* 57: 305–313.
6. Murata, H., and S. Naoe. 1987. Experimental *Candida*-induced arteritis in mice—relation to arteritis in Kawasaki disease. *Prog. Clin. Biol. Res.* 250: 523.
7. Takahashi, K., T. Oharaseki, M. Wakayama, Y. Yokouchi, S. Naoe, and H. Murata. 2004. Histopathological features of murine systemic vasculitis caused by *Candida albicans* extract—an animal model of Kawasaki Disease. *Inflamm. Res.* 53: 72–77.
8. Ohno, N. 2008. A murine model of vasculitis induced by fungal polysaccharide. *Cardiovasc. Hematol. Agents Med. Chem.* 6: 44–52.
9. Ohno, N. 2006. Models of Kawasaki disease. *Drug Discov. Today Dis. Models* 3: 83–89.
10. Hirata, N., K. Ishibashi, S. Ohta, S. Hata, H. Shinohara, M. Kitamura, N. Miura, and N. Ohno. 2006. Histopathological examination and analysis of mortality in DBA/2 mouse vasculitis induced with CAWS, a water-soluble extracellular polysaccharide fraction obtained from *Candida albicans*. *Yakugaku Zasshi* 126: 643–650.
11. Nagi-Miura, N., Y. Shingo, Y. Adachi, A. Ishida-Okawara, T. Oharaseki, K. Takahashi, S. Naoe, K. Suzuki, and N. Ohno. 2004. Induction of coronary arteritis with administration of CAWS (*Candida albicans* water-soluble fraction) depending on mouse strains. *Immunopharmacol. Immunotoxicol.* 26: 527–543.
12. Kurihara, K., N. N. Miura, M. Uchiyama, N. Ohno, Y. Adachi, M. Aizawa, H. Tamura, S. Tanaka, and T. Yadomae. 2000. Measurement of blood clearance time by Limulus G test of *Candida*-water soluble polysaccharide fraction, CAWS, in mice. *FEMS Immunol. Med. Microbiol.* 29: 69–76.
13. Kurihara, K., Y. Shingo, N. N. Miura, S. Horie, Y. Usui, Y. Adachi, T. Yadomae, and N. Ohno. 2003. Effect of CAWS, a mannoprotein-β-glucan complex of *Candida albicans*, on leukocyte, endothelial cell, and platelet functions in vitro. *Biol. Pharm. Bull.* 26: 233–240.
14. Nagi-Miura, N., T. Harada, H. Shinohara, K. Kurihara, Y. Adachi, A. Ishida-Okawara, T. Oharaseki, K. Takahashi, S. Naoe, K. Suzuki, and N. Ohno. 2006. Lethal and severe coronary arteritis in DBA/2 mice induced by fungal pathogen, CAWS. *Candida albicans* water-soluble fraction. *Atherosclerosis* 186: 310–320.
15. Ishida-Okawara, A., N. Nagi-Miura, T. Oharaseki, K. Takahashi, A. Okumura, H. Tachikawa, S. Kashiwamura, H. Okamura, N. Ohno, H. Okada, et al. 2007. Neutrophil activation and arteritis induced by *C. albicans* water-soluble mannoprotein-β-glucan complex (CAWS). *Exp. Mol. Pathol.* 82: 220–226.
16. Kanegane, H., K. Nomura, T. Futatani, and T. Miyawaki. 2002. Intravenous immunoglobulin replacement therapy in X-linked agammaglobulinemia (in Japanese; includes abstract). *Jpn. J. Clin. Immun.* 25: 337–343.
17. Berning, A. K., E. M. Eicher, W. E. Paul, and I. Scher. 1980. Mapping of the X-linked immune deficiency mutation (*xid*) of CBA/N mice. *J. Immunol.* 124: 1875–1877.
18. Cancro, M. P., A. P. Sah, S. L. Levy, D. M. Allman, M. R. Schmidt, and R. T. Woodland. 2001. *xid* mice reveal the interplay of homeostasis and Bruton's tyrosine kinase-mediated selection at multiple stages of B cell development. *Int. Immunol.* 13: 1501–1514.
19. Middendorp, S., G. M. Dingjan, A. Maas, K. Dahlenborg, and R. W. Hendriks. 2003. Function of Bruton's tyrosine kinase during B cell development is partially independent of its catalytic activity. *J. Immunol.* 171: 5988–5996.
20. Satterthwaite, A. B., and O. N. Witte. 2000. The role of Bruton's tyrosine kinase in B cell development and function: a genetic perspective. *Immunol. Rev.* 175: 120–127.
21. Mukhopadhyay, S., M. Mohanty, A. Mangla, A. George, V. Bal, S. Rath, and B. Ravindran. 1999. Bruton's tyrosine kinase deficiency in macrophages inhibits nitric oxide generation leading to enhancement of IL-12 induction. *J. Immunol.* 163: 1786–1792.
22. Koike, M., Y. Kikuchi, A. Tominaga, S. Takaki, K. Akagi, J. Miyazaki, K. Yamamura, and K. Takatsu. 1995. Defective IL-5-receptor-mediated signaling in B cells of X-linked immunodeficient mice. *Int. Immunol.* 7: 21–30.
23. Moore, K. W., R. de Waal Malefyt, R. L. Coffman, and A. O'Garra. 2001. Interleukin-10 and the interleukin-10 receptor. *Annu. Rev. Immunol.* 19: 683–765.
24. Senzaki, H., S. Masutani, J. Kobayashi, T. Kobayashi, H. Nakano, H. Nagasaka, N. Sasaki, H. Asano, S. Kyo, and Y. Yokote. 2004. Circulating matrix metalloproteinases and their inhibitors in patients with Kawasaki disease. *Circulation* 104: 860–863.
25. Chua, P. K., M. E. Melish, Q. Yu, R. Yanagihara, K. S. Yamamoto, and V. R. Nerurkar. 2003. Elevated levels of matrix metalloproteinase 9 and tissue inhibitor of metalloproteinase 1 during the acute phase of Kawasaki disease. *Clin. Diagn. Lab. Immunol.* 10: 308–314.
26. Gavin, P. J., S. E. Crawford, S. T. Shulman, F. L. Garcia, and A. H. Rowley. 2003. Systemic arterial expression of matrix metalloproteinases 2 and 9 in acute Kawasaki disease. *Arterioscler. Thromb. Vasc. Biol.* 23: 576–581.
27. Jefferies, C. A., and L. A. O'Neill. 2004. Bruton's tyrosine kinase (Btk)—the critical tyrosine kinase in LPS signalling? *Immunol. Lett.* 92: 15–22.
28. Shinohara, H., N. Nagi-Miura, K. Ishibashi, Y. Adachi, A. Ishida-Okawara, T. Oharaseki, K. Takahashi, S. Naoe, K. Suzuki, and N. Ohno. 2006. β-Mannosyl linkages negatively regulate anaphylaxis and vasculitis in mice, induced by CAWS, fungal PAMPs composed of mannoprotein-β-glucan complex secreted by *Candida albicans*. *Biol. Pharm. Bull.* 29: 1854–1861.
29. Mikami, T., K. Fukushi, M. Ishitani, K. Ishitani, S. Suzuki, and M. Suzuki. 1991. Induction of platelet-activating factor in mice by intravenous administration of a neutral fraction of bakers' yeast mannan. *Lipids* 26: 1404–1407.
30. Zhang, Q., N. Mousdicas, Q. Yi, M. Al-Hassani, S. D. Billings, S. M. Perkins, K. M. Howard, S. Ishii, T. Shimizu, and J. B. Travers. 2005. Staphylococcal lipoteichoic acid inhibits delayed-type hypersensitivity reactions via the platelet-activating factor receptor. *J. Clin. Invest.* 115: 2855–2861.
31. Pei, Y., L. A. Barber, R. C. Murphy, C. A. Johnson, S. W. Kelley, L. C. Dy, R. H. Fertel, T. M. Nguyen, D. A. Williams, and J. B. Travers. 1998. Activation of the epidermal platelet-activating factor receptor results in cytokine and cyclooxygenase-2 biosynthesis. *J. Immunol.* 161: 1954–1961.
32. Dy, L. C., Y. Pei, and J. B. Travers. 1999. Augmentation of ultraviolet B radiation-induced tumor necrosis factor production by the epidermal platelet-activating factor receptor. *J. Biol. Chem.* 274: 26917–26921.
33. Southall, M. D., J. S. Isenberg, H. Nakshatri, Q. Yi, Y. Pei, D. F. Spandau, and J. B. Travers. 2001. The platelet-activating factor receptor protects epidermal cells from tumor necrosis factor (TNF) α and TNF-related apoptosis-inducing ligand-induced apoptosis through an NF-κB-dependent process. *J. Biol. Chem.* 276: 45548–45554.
34. Walterscheid, J. P., S. E. Ullrich, and D. X. Nghiem. 2002. Platelet-activating factor, a molecular sensor for cellular damage, activates systemic immune suppression. *J. Exp. Med.* 195: 171–179.

BMC Genetics

BioMed Central

Research article

Open Access

Development of an integrative database with 499 novel microsatellite markers for *Macaca fascicularis*

Atsunori Higashino[1], Naoki Osada[2], Yumiko Suto[3], Makoto Hirata[2], Yosuke Kameoka[2], Ichiro Takahashi[2] and Keiji Terao*[1]

Address: [1]Tsukuba Primate Research Center, National Institute of Biomedical Innovation, 1-1 Hachimandai, Tsukuba, Ibaraki 305-0843, Japan, [2]Department of Biomedical Resources, National Institute of Biomedical Innovation, 7-6-8 Saito-Asagi, Ibaraki, Osaka 567-0085, Japan and [3]Department of Research and Development, Central Blood Institute, Japanese Red Cross Society, 2-1-67 Tatsumi, Koto-ku, Tokyo 135-8521, Japan

Email: Atsunori Higashino - higashino@nibio.go.jp; Naoki Osada - nosada@nibio.go.jp; Yumiko Suto - y-suto@bs.jrc.or.jp; Makoto Hirata - mhirata@nibio.go.jp; Yosuke Kameoka - ykameoka@nibio.go.jp; Ichiro Takahashi - ichiro-t@nibio.go.jp; Keiji Terao* - terao@nibio.go.jp

* Corresponding author

Published: 5 June 2009

BMC Genetics 2009, **10**:24 doi:10.1186/1471-2156-10-24

Received: 18 December 2008
Accepted: 5 June 2009

This article is available from: http://www.biomedcentral.com/1471-2156/10/24

Abstract

Background: Cynomolgus macaques (*Macaca fascicularis*) are a valuable resource for linkage studies of genetic disorders, but their microsatellite markers are not sufficient. In genetic studies, a prerequisite for mapping genes is development of a genome-wide set of microsatellite markers in target organisms. A whole genome sequence and its annotation also facilitate identification of markers for causative mutations. The aim of this study is to establish hundreds of microsatellite markers and to develop an integrative cynomolgus macaque genome database with a variety of datasets including marker and gene information that will be useful for further genetic analyses in this species.

Results: We investigated the level of polymorphisms in cynomolgus monkeys for 671 microsatellite markers that are covered by our established Bacterial Artificial Chromosome (BAC) clones. Four hundred and ninety-nine (74.4%) of the markers were found to be polymorphic using standard PCR analysis. The average number of alleles and average expected heterozygosity at these polymorphic loci in ten cynomolgus macaques were 8.20 and 0.75, respectively.

Conclusion: BAC clones and novel microsatellite markers were assigned to the rhesus genome sequence and linked with our cynomolgus macaque cDNA database (QFbase). Our novel microsatellite marker set and genomic database will be valuable integrative resources in analyzing genetic disorders in cynomolgus macaques.

Background

Cynomolgus macaques (*Macaca fascicularis*) are one of the most commonly used nonhuman primates in biomedical research. Currently, about two thousand cynomolgus macaques are maintained in Tsukuba Primate Research Center (TPRC), Japan [1]. Several lineages of the captive cynomolgus macaques have genetic disorders such as macular degeneration [2] and endometriosis [3]. In genetic studies, a prerequisite for mapping genes is development of a genome-wide set of microsatellite markers in target organisms. A whole genome sequence and its annotation also facilitate identification of markers for causative

mutations. A comprehensive cynomolgus macaque genome database, including a map of Bacterial Artificial Chromosome (BAC) clones, 5'-end expressed sequence tags (ESTs), microsatellite markers, primer sequences for microsatellite markers, and genes around the microsatellite markers would be valuable for linkage analyses, but, unfortunately, complete genome of cynomolgus macaque is not yet sequenced.

A microsatellite marker set is a versatile tool that would assist in colony management, conservation work, and paternity testing of nonhuman primates [4-12]. Microsatellite markers of human [13] and some nonhuman primate species [14-17] are now widely available, facilitating linkage analyses in these species. The first generation of genetic linkage maps of baboons [18,19] and rhesus macaques were developed by Rogers, *et al.* [20]. However, few studies have been conducted on microsatellite markers in cynomolgus macaques [12,21]. In this study, we established 499 microsatellite markers that were covered by pre-identified Bacterial Artificial Chromosome (BAC) clones for cynomolgus macaques. We also developed an integrative cynomolgus macaque genome database with a variety of datasets including marker and gene information that will be useful for further genetic analyses in this species. Advantages of this study are (1) since most of newly developed microsatellite marker loci were covered by the BAC clones, we could search for their chromosomal locations by *in silico* mapping, (2) these microsatellite markers were mapped to the rhesus macaque genome sequence http://genebank.nibio.go.jp/cgi-bin/gbrowse/rheMac2/, and (3) the 499 novel markers established in this study outnumber the previously reported microsatellite markers in other macaques and are probably useful for linkage studies in other non-human primate species as well.

At a genome-wide level, the cynomolgus and rhesus macaque genomes are very similar; their genetic divergence is about 0.4% at a nucleotide level [22]. In addition, their karyotypes are also very similar [23]. To design cynomolgus macaque microsatellite markers based on the rhesus macaque genome sequence would be a reasonable and efficient way of establishing a species-specific genomic conformation for this species. The development of a linkage map in this species is a first step toward exploring the genes responsible for genetic disorders in captive macaques.

Results

Identification of polymorphic microsatellite and construction of microsatellite marker database for cynomolgus macaque

BAC-end sequences of 768 clones of a cynomolgus macaque were determined. Of these, 487 BAC clones were successfully mapped onto the draft rhesus genome sequence (see method). Within the regions that were covered by the BAC clones, we selected 671 candidate loci from 394 BAC clones that harbor dinucleotide repeats equal or longer than 20 bp in the rhesus genome sequence. Of these, 34 markers were selected from rhesus macaque or human microsatellite markers identified by previous studies [13,24-28]. Our marker set does not contain the markers previously developed by Kikuchi *et al.* [21]. These primer sequences and their genomic locations are presented in Additional file 1.

Next, we investigated whether these candidate repeats for microsatellite markers are polymorphic using 10 unrelated cynomolgus macaque individuals from Indonesia, Malaysia, and the Philippines. Of the 671 microsatellite markers tested, 499 (74.4%) gave rise to polymorphic PCR products, approximately the same size as expected from the rhesus or human genome sequence. The detailed information is presented in Additional file 1 and also on our website http://genebank.nibio.go.jp/cgi-bin/qfbase/macMMarker.cgi/. Because some of the microsatellite markers located on very close loci, which were covered by single BAC clone, we estimated the coverage of the genome by the microsatellite makers using only one polymorphic microsatellite marker which have the distance at least 0.1 Mbp between neighboring markers. The average distance between newly developed markers was about 10 cM, assuming that the macaque genome comprised 3000 Mbp of nucleotides. PCR product sizes are 63–647 bp with an average size of 247 bp. The average number of alleles per polymorphic marker was 8.20 (range 2–17) and the average expected heterozygosity was 0.75 (range 0.10–0.94) for these 499 markers in the cynomolgus macaques. The distribution of expected heterozygosity values showed that a substantial number of the markers have expected heterozygosity greater than 0.80. Microsatellite markers with expected heterozygosity > 0.75 are regarded as highly polymorphic [20]. According to this criterion, 324 of 499 markers (64.9%) were highly polymorphic (Figure 1). In order to check the mode of inheritance of these markers, we investigated additional four families consisting of 27 animals to confirm the inheritance of 453 autosomal markers and found that 412 markers showed no contradictions concerning Mendelian inheritance (see Additional file 2).

We investigated the distribution of the microsatellite markers on the human and rhesus chromosomes. As shown in Table 1, the novel microsatellite markers were distributed over all autosomes and X-chromosome of both species. Since the draft genome sequence of the rhesus Y-chromosome is not available, we did not obtain microsatellite markers on the Y-chromosome.

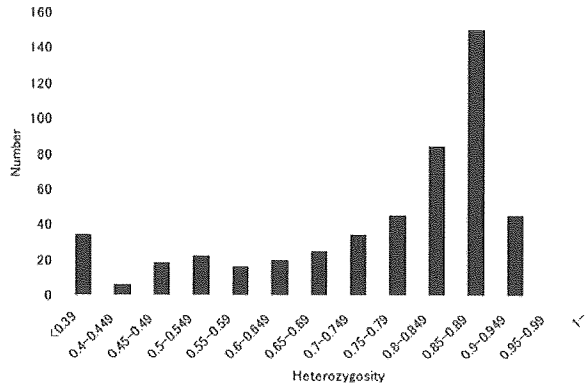

Figure 1
Distribution of heterozygosity for the 499 microsatellite markers. Heterozygosities (H_e) range from 0.10 to 0.94, with a mean of 0.75. Among 499 polymorphic markers, 324 (64.9%) had $H_e > 0.75$.

Construction of integrative cynomolgus macaque genome database

We further constructed a genome browser for cynomolgus macaques, based on the rhesus genome sequence. In this database, users can search the positions of cynomolgus macaque BAC clones, 5'-end expressed sequence tags (ESTs) and microsatellite markers on the rhesus macaque genome. In addition, human and macaque cDNA sequences and rhesus macaque genes predicted by Ensembl [29] were aligned on the genome. This database is also connected to QFbase, which contains data of more than 130,000 cynomolgus macaque cDNAs [22]. This information will facilitate the search for known or predicted cynomolgus macaque genes near the microsatellite markers and help to narrow down candidate regions for functional genes near these markers identified by linkage analysis. The address of the database is http://genebank.nibio.go.jp/cgi-bin/gbrowse/rheMac2/.

Discussion

At present, a few microsatellite markers have been reported for cynomolgus macaques [12,21] even though the microsatellite tool would be valuable for studying cynomolgus macaque genetic diseases. In this work, we have designed 637 primer pairs and selected 34 primer pairs from NCBI/UniSTS. Of the 671 marker candidates, 499 polymorphic microsatellite markers located on cynomolgus macaque BAC clones. These polymorphic markers could be amplified with high probability with the same protocol as for human microsatellite markers used for other macaques [16,20]. Most of the developed microsatellite markers have high expected heterozygosity and are distributed throughout the human and rhesus macaque chromosomes. Our microsatellite marker set will be available for various studies in macaques, and macaque chromosomal information of developed microsatellite markers is also available from the following database http://genebank.nibio.go.jp/cgi-bin/gbrowse/rheMac2/. These BAC clones will be helpful for further identification and functional analysis of genes implicated in genetic disorders.

In the genome database of cynomolgus macaques, we assumed that the synteny of the cynomolgus and rhesus macaques is highly conserved. Although previous studies suggested that their chromosomes were highly similar at a microscopic level, smaller translocations, insertions or deletions may exist between the two genomes [22,23]. The BAC resource can be used to verify such genomic differences by fluorescent *in situ* hybridization (FISH) method. We verified the suitability of such mapping by FISH with 12 BAC clones. Although mapping all BAC clones by FISH is not a practical approach, we are able to check the synteny between the two genomes when a particularly interesting locus is found by further studies (see Additional file 3).

In the polymorphism analysis, all PCR products showed high fluorescence intensities, indicating the presence of ample labeled PCR product, even without optimization. Optimization of annealing temperature and magnesium concentration for the unsuccessful markers using cynomolgus macaque DNA would certainly yield additional useful markers. In addition, many of the microsatellite polymorphisms reported here will also be useful in other macaques [30,31].

Currently, about 800 human microsatellite markers, which cover all areas of the human genome with intervals of 5 cM, are commercially available. Rogers *et al.* developed the first generation of genetic linkage maps of baboons [18,19] and rhesus macaques [20], primarily consisting of human microsatellite loci amplified using the published human PCR primers. Human markers have been tested in the baboons, and over 280 microsatellites were used in studies for osteoporosis in this species [32,33]. The 499 novel markers established in this study outnumber the previously reported microsatellite markers in baboons and rhesus monkeys and are probably useful for linkage studies in other non-human primate species as well. These microsatellite markers are also valuable resources for the management of captive macaque colonies.

We are currently using linkage analysis to identify genetic loci implicated in hereditary macular degeneration in cynomolgus macaques, which is the only animal model of human age-related macular degeneration. Early onset macular degeneration occurred spontaneously in certain

Table 1: Microsatellite marker distribution on rhesus macaque and human chromosomes.

Rhesus chromosome	Human chromosome	Microsatellite number
1	1	37
12	2	17
13	2	30
2	3	35
5	4	27
6	5	28
4	6	25
3	7	36
8	8	18
15	9	10
9	10	22
14	11	22
11	12	33
17	13	27
7	14	12
7	15	15
20	16	15
16	17	10
18	18	18
19	19	8
10	20	7
3	21	7
10	22	14
X	X	26

cynomolgus macaque families at the Tsukuba Primate Research Center (TPRC), and family analysis revealed that this disease is controlled by autosomal dominant genes [2]. The integration of various genetic tools including our database would greatly facilitate the genetic-based research on disease models in the future. We should note that, however, the whole genome association studies, especially for candidate genes with only minor effects, might require a far denser map than that reported here.

Conclusion

Cynomolgus macaques (*Macaca fascicularis*) are one of the most commonly used nonhuman primates in biomedical research. In this study, we established 499 microsatellite markers for cynomolgus macaques. We also developed an integrative cynomolgus macaque genome database with a variety of datasets that will be useful for further genetic analyses in this species. The development of a linkage map in this species is a first step toward exploring the genes responsible for genetic disorders in captive macaques. These datasets are definitely valuable to many researchers who are in the field of primate genetics.

Methods

DNA sampling and pedigree structure

Whole blood samples were obtained from 37 pedigreed cynomolgus macaques, aged 3–29 years, consisting of 17 males and 20 females housed at the TPRC, National Institute of Biomedical Innovation (NIBIO), Tsukuba, Japan. Blood samples of 10 unrelated individuals (four males and six females) were used for the polymorphism analysis. They consist of three Indonesian, four Philippine, and three Malaysian cynomolgus macaques. Blood samples of 27 individuals in four families (13 males and 14 females) from Malaysian cynomolgus macaques were used for the inheritance analysis. Genomic DNA was isolated from 10 ml of heparinized peripheral blood using the Wizard Genomic DNA purification kit (Promega, WI, USA). These macaques were cared for and handled according to guidelines established by the Institutional Animal Care and Use Committee of the NIBIO and the standard operating procedures for macaques at the TPRC. Collection of the blood was conducted in accordance with all guidelines required in the Laboratory Biosafety Manual, World Health Organization at the TPRC.

BAC library and BAC-end sequence

We used a BAC library that was constructed using DNA from renal cells of cynomolgus macaques. The library consists of approximately 110,000 recombinant BAC clones providing 3.4-fold coverage of the cynomolgus macaque genome. The cynomolgus macaque BAC library was obtained from the Department of Biomedical Resources, National Institute of Biomedical Innovation, Osaka, Japan. DNA sequencing was performed with BigDye Terminator v3.1 Ready Reaction Mix and ABI Prism-Avant Genetic Analyzer (Applied Biosystems, CA, USA).

In silico *mapping of the BAC-end sequences on the rhesus macaquegenome*

The BAC-end sequences were mapped onto the draft genome sequence of rhesus macaques (rheMac2 assembly) using a BLAST program ($E = 10^{-30}$). Repeat sequences were masked before the BLAST search. When the two BAC-end sequences from the same BAC clone were aligned as head-to-head directions within the range of 10–300 kb on the rhesus genome draft sequences, we assumed that the BAC clone was correctly assigned to the genome. In order to choose candidate loci for microsatellite markers within the region, we surveyed short tandem repeats (STRs) spanning at least 20 nucleotides, with motif length 2 (i.e., CACACA-nucleotide repeats), which was identified using Tandem repeats finder software [34].

Primer design and PCR

For 637 microsatellite loci on sequenced BAC clones, paired primers were designed using DNASIS software (Hitachi Software Engineering, Tokyo, Japan). The primer sets were confirmed not to match more than one region of the rhesus genome draft sequence [35]. MFA0028-0061 markers were selected from the NCBI/UniSTS id: markers and mapping data are 72106, 147912, 8379, 63879,

13743, 19265, 181717, 37796, 74733, 256705, 75673, 10546, 264996, 153124, 73737, 65585, 148897, 9343, 22659, 42001, 46786, 41570, 78383, 13963, 147924, 83050, 46652, 148707, 11528, 89846, 30829, 94606, 94603, and 76519, respectively [13,24-28]. The forward primers were labeled with one of three fluorescent dyes, 6-FAM, HEX, or NED. Amplification was done in a 384-well format on the 9700 Thermal Cyclers (Applied Biosystems, CA, USA). Ten microliters of the reaction mixture contained 10 ng of genomic DNA, 2.5 nmol each of dATP, dCTP, dGTP, and dTTP, 0.25 units of ExTaq, 5.0 pmol of forward and reverse primers, and the manufacturer's PCR buffer (all purchased from Takara Biosystems, Otsu, Japan). Cycling conditions are as follows: an initial denaturation was performed at 94°C for 5 min, 30 cycles of amplification were performed at 94°C for 1 min, 55°C for 1 min, and 72°C for 1 min, and one cycle of extension was performed at 72°C for 7 min. The same PCR conditions were applied to all amplifications.

Analyses of microsatellite polymorphisms and genetic inheritances

Amplified PCR products were mixed with gel-loading cocktails containing deionized formamide and labeled size standards (GeneMapper-LIZ 500; Applied Biosystems, CA, USA). Samples were run on the Applied Biosystems 3730 DNA analyzer (Applied Biosystems, CA, USA). Expected heterozygosity (H_e) of loci was calculated using the formula: $H_e = 1 - \sum p^2_i$ [36]. We examined expected heterozygosity according to Nei [37]. Using 453 autosomal markers, genetic inheritance analyses were performed by checkfam [38].

Database construction

The cynomolgus macaque genome database was constructed using the rhesus genome sequence (rheMac2 assembly) as a reference. Information on microsatellite markers, BAC clones, 130,000 5'-end expressed sequence tags (ESTs) and annotation of genes was visualized with Generic Genome Browser (GBrowse) software [39]. The annotation of human and macaque transcripts on the genome was retrieved from the UCSC genome browser [40].

Availability and requirements

Database name: QFbase-GBrowse

Database home page: http://genebank.nibio.go.jp/cgi-bin/gbrowse/rheMac2/

Any restrictions to use by non-academics: no restriction

Authors' contributions

AH, NO, YS, and KT contributed to the designing of the research. AH, NO, YS, YK, and IT performed the experiments and analyzed the data. NO and MH contributed to the database construction. AH, NO, YS, and KT wrote the manuscript. All authors read and approved the final manuscript.

Additional material

Additional file 1

List of 671 primer pairs for microsatellite candidate loci. *Polymorphism was determined with ten unrelated macaques. Chr, Chromosome; Y, amplification; N, no amplification; P, polymorphic; M, monomorphic. These data are also available at our website http://genebank.nibio.go.jp/cgi-bin/qfbase/macMMarker.cgi, and these microsatellite markers are mapped to the rhesus macaque genome database http://genebank.nibio.go.jp/cgi-bin/gbrowse/rheMac2/. MFA0028-0061 markers are reported as NCBI/UniSTS id: markers and mapping data are 72106, 147912, 8379, 63879, 13743, 19265, 181717, 37796, 74733, 256705, 75673, 10546, 264996, 153124, 73737, 65585, 148897, 9343, 22659, 42001, 46786, 41570, 78383, 13963, 147924, 83050, 46652, 148707, 11528, 89846, 30829, 94606, 94603, and 76519, respectively.*

Click here for file
[http://www.biomedcentral.com/content/supplementary/1471-2156-10-24-S1.xls]

Additional file 2

Allele data of 453 polymorphic markers. *We checked the mode of inheritance of 453 microsatellite markers in four families (13 males and 14 females) from Malaysian cynomolgus macaques. Of these, 412 markers showed no contradictions concerning Mendelian inheritance.*

Click here for file
[http://www.biomedcentral.com/content/supplementary/1471-2156-10-24-S2.xls]

Additional file 3

Chromosomal localization of cynomolgus macaque BAC clones. *Chromosome numbers are (A): 11, 12, (B): 17, 13, (C): 7, 15, and (D): 19, 19, macaques (cynomolgus and rhesus) and human, respectively. Green spots indicate hybridization signals of BAC DNA. Background staining (red) is propidium iodide (PI).*

Click here for file
[http://www.biomedcentral.com/content/supplementary/1471-2156-10-24-S3.doc]

Acknowledgements

This work was supported by KHB1202 to KT from the Japan Health Sciences Foundation and H19-Bio-Shitei-004 to NO, YK, IT, KT from the Ministry of Health, Labor, and Welfare, Japan.

References

1. Suzuki MT, Ono T, Kohno M, Ogawa H: **Hour of Delivery in Cynomolgus Monkeys Under Indoor Individually-caged Conditions.** *Primates* 1990, **31**:251-255.
2. Suzuki MT, Terao K, Yoshikawa Y: **Familial early onset macular degeneration in cynomolgus monkeys (*Macaca fascicularis*).** *Primates* 2003, **44**:291-294.
3. Ami Y, Suzaki Y, Goto N: **Endometriosis in cynomolgus monkeys retired from breeding.** *J Vet Med Sci* 1993, **55**:7-11.
4. Smith DG: **Use of genetic markers in the colony management of nonhuman primates: a review.** *Lab Anim Sci* 1982, **32**:540-546.

5. Inoue M, Takenaka O: **Japanese Macaque Microsatellite PCR Primers for Paternity Testing.** *Primates* 1993, **34**:37-45.
6. Kanthaswamy S, Smith DG: **Use of Microsatellite Polymorphisms for Paternity Exclusion in Rhesus Macaques (*Macaca mulatta*).** *Primates* 1998, **39**:135-145.
7. Nurnberg P, Sauermann U, Kayser M, Lanfer C, Manz E, Widdig A, Berard J, Bercovitch FB, Kessler M, Schmidtke J, Krawczak M: **Paternity assessment in rhesus macaques (*Macaca mulatta*): multilocus DNA fingerprinting and PCR marker typing.** *Am J Primatol* 1998, **44**:1-18.
8. Smith DG, Kanthaswamy S, Viray J, Cody L: **Additional highly polymorphic microsatellite (STR) loci for estimating kinship in rhesus macaques (*Macaca mulatta*).** *Am J Primatol* 2000, **50**:1-7.
9. Oka T, Takenaka O: **Wild Gibbon's Parentage Tested by Non-invasive DNA Sampling and PCR-amplified Polymorphic Microsatellites.** *Primates* 2001, **42**:67-73.
10. Lavergne A, Catzeflis F, Lacote S, Barnaud A, Bordier M, Mercereau-Puijalon O, Contamin H: **Genetic analysis of the *Saimiri* breeding colony of the Pasteur Institute (French Guiana): development of a molecular typing method using a combination of nuclear and mitochondrial DNA markers.** *J Med Primatol* 2003, **32**:330-340.
11. Andrade MCR, Penedo MCT, Ward T, Silva VF, Bertolini LR, Roberts JA, Leite JPG, Cabello PH: **Determination of genetic status in a closed colony of rhesus monkeys (*Macaca mulatta*).** *Primates* 2004, **45**:183-186.
12. Kanthaswamy S, Satkoski J, George D, Kou A, Erickson BJ-A, Smith DG: **Interspecies Hybridization and the Stratification of Nuclear Genetic Variation of Rhesus (*Macaca Mulatta*) and Long-Tailed Macaques (*Macaca Fascicularis*).** *Int J Primatol* 2008, **29**:1295-1311.
13. Dib C, Faure S, Fizames C, Samson D, Drouot N, Vignal A, Millasseau P, Marc S, Hazan J, Seboun E, Lathrop M, Gyapay G, Morissette J, Weissenbach J: **A comprehensive genetic map of the human genome based on 5,264 microsatellites.** *Nature* 1996, **380**:152-154.
14. Chu J-H, Wu H-Y, Yang Y-J, Takenaka O, Lin Y-S: **Polymorphic Microsatellite Loci and Low-invasive DNA Sampling in *Macaca cyclopis*.** *Primates* 1999, **40**:573-580.
15. Nair S, Ha J, Rogers J: **Nineteen New Microsatellite DNA Polymorphisms in Pigtailed Macaques (*Macaca nemestrina*).** *Primates* 2000, **41**:343-350.
16. Hadfield RM, Pullen JG, Davies KF, Wolfensohn SE, Kemnitz JW, Weeks DE, Bennett ST, Kennedy SH: **Toward developing a genome-wide microsatellite marker set for linkage analysis in the rhesus macaque (*Macaca mulatta*): identification of 76 polymorphic markers.** *Am J Primatol* 2001, **54**:223-231.
17. Rogers J, Bergstrom M, Garcia R 4th, Kaplan J, Arya A, Novakowski L, Johnson Z, Vinson A, Shelledy W: **A panel of 20 highly variable microsatellite polymorphisms in rhesus macaques (*Macaca mulatta*) selected for pedigree or population genetic analysis.** *Am J Primatol* 2005, **67**:377-383.
18. Rogers J, Witte SM, Kammerer CM, Hixson JE, MacCluer JW: **Linkage mapping in *Papio* baboons: conservation of a syntenic group of six markers on human chromosome 1.** *Genomics* 1995, **28**:251-254.
19. Rogers J, Mahaney MC, Witte SM, Nair S, Newman D, Wedel S, Rodriguez LA, Rice KS, Slifer SH, Perelygin A, Slifer M, Palladino-Negro P, Newman T, Chambers K, Joslyn G, Parry P, Morin PA: **A genetic linkage map of the baboon (*Papio hamadryas*) genome based on human microsatellite polymorphisms.** *Genomics* 2000, **67**:237-247.
20. Rogers J, Garcia R, Shelledy W, Kaplan J, Arya A, Johnson Z, Bergstrom M, Novakowski L, Nair P, Vinson A, Newman D, Heckman G, Cameron J: **An initial genetic linkage map of the rhesus macaque (*Macaca mulatta*) genome using human microsatellite loci.** *Genomics* 2006, **87**:30-38.
21. Kikuchi T, Hara M, Terao K: **Development of a microsatellite marker set applicable to genome-wide screening of cynomolgus monkeys (*Macaca fascicularis*).** *Primates* 2007, **48**:140-146.
22. Osada N, Hashimoto K, Kameoka Y, Hirata M, Tanuma R, Uno Y, Inoue I, Hida M, Suzuki Y, Sugano S, Terao K, Kusuda J, Takahashi I: **Large-scale analysis of *Macaca fascicularis* transcripts and inference of genetic divergence between *M. fascicularis* and *M. mulatta*.** *BMC Genomics* 2008, **9**:90.
23. Dutrillaux B, Biemont MC, Viegas-Pequignot E, Laurent C: **Comparison of the karyotypes of four Cercopithecoidae: *Papio papio, P. anubis, Macaca mulatta*, and *M. fascicularis*.** *Cytogenet Cell Genet* 1979, **23**:77-83.
24. Weber JL, May PE: **Abundant class of human DNA polymorphisms which can be typed using the polymerase chain reaction.** *Am J Hum Genet* 1989, **44**:388-396.
25. Marineau C, Rouleau GA: **Dinucleotide repeat polymorphism at the human CRYB2 gene locus (22q11.2).** *Nucleic Acids Res* 1992, **20**:1430.
26. Weissenbach J, Gyapay G, Dib C, Vignal A, Morissette J, Millasseau P, Vaysseix G, Lathrop M: **A second-generation linkage map of the human genome.** *Nature* 1992, **359**:794-801.
27. Gyapay G, Morissette J, Vignal A, Dib C, Fizames C, Millasseau P, Marc S, Bernardi G, Lathrop M, Weissenbach J: **The 1993–94 Genethon human genetic linkage map.** *Nat Genet* 1994, **7**:246-339.
28. Feinstein E, Druck T, Kastury K, Berissi H, Goodart SA, Overhauser J, Kimchi A, Huebner K: **Assignment of DAP1 and DAPK – genes that positively mediate programmed cell death triggered by IFN-gamma – to chromosome regions 5p12.2 and 9q34.1, respectively.** *Genomics* 1995, **29**:305-307.
29. Hubbard T, Barker D, Birney E, Cameron G, Chen Y, Clark L, Cox T, Cuff J, Curwen V, Down T, Durbin R, Eyras E, Gilbert J, Hammond M, Huminiecki L, Kasprzyk A, Lehvaslaiho H, Lijnzaad P, Melsopp C, Mongin E, Pettett R, Pocock M, Potter S, Rust A, Schmidt E, Searle S, Slater G, Smith J, Spooner W, Stabenau A, Stalker J, Stupka E, Ureta-Vidal A, Vastrik I, Clamp M: **The Ensembl genome database project.** *Nucleic Acids Res* 2002, **30**:38-41.
30. Blanquer-Maumont A, Crouau-Roy B: **Polymorphism, monomorphism, and sequences in conserved microsatellites in primate species.** *J Mol Evol* 1995, **41**:492-497.
31. Domingo-Roura X, Lopez-Giraldez T, Shinohara M, Takenaka O: **Hypervariable microsatellite loci in the Japanese macaque (*Macaca fuscata*) conserved in related species.** *Am J Primatol* 1997, **43**:357-360.
32. Rogers J, Hixson JE: **Baboons as an animal model for genetic studies of common human disease.** *Am J Hum Genet* 1997, **61**:489-493.
33. Morin PA, Mahboubi P, Wedel S, Rogers J: **Rapid screening and comparison of human microsatellite markers in baboons: allele size is conserved, but allele number is not.** *Genomics* 1998, **53**:12-20.
34. Benson G: **Tandem repeats finder: a program to analyze DNA sequences.** *Nucleic Acids Res* 1999, **27**:573-580.
35. **The UCSC Genome Browser Database** [http://genome.ucsc.edu/]
36. Nei M, Roychoudhury AK: **Sampling variances of heterozygosity and genetic distance.** *Genetics* 1974, **76**:379-390.
37. Nei M: *Molecular evolutionary genetics* New York: Columbia University Press; 1987.
38. Saito M, Saito A, Kamatani N: **Web-based detection of genotype errors in pedigree data.** *J Hum Genet* 2002, **47**:377-379.
39. Stein LD, Mungall C, Shu SQ, Caudy M, Mangone M, Day A, Nickerson E, Stajich JE, Harris TW, Arva A, Lewis S: **The generic genome browser: a building block for a model organism system database.** *Genome Res* 2002, **12**:1599-1610.
40. Karolchik D, Baertsch R, Diekhans M, Furey TS, Hinrichs A, Lu YT, Roskin KM, Schwartz M, Sugnet CW, Thomas DJ, Weber RJ, Haussler D, Kent WJ: **The UCSC Genome Browser Database.** *Nucleic Acids Res* 2003, **31**:51-54.

Genes to Cells

Efficient reprogramming of human and mouse primary extra-embryonic cells to pluripotent stem cells

Shogo Nagata[1,2], Masashi Toyoda[3], Shinpei Yamaguchi[1], Kunio Hirano[1], Hatsune Makino[3], Koichiro Nishino[3], Yoshitaka Miyagawa[4], Hajime Okita[4], Nobutaka Kiyokawa[4], Masato Nakagawa[5], Shinya Yamanaka[5], Hidenori Akutsu[3], Akihiro Umezawa[3] and Takashi Tada[1,2]*

[1]*Stem Cell Engineering, Institute for Frontier Medical Sciences, Kyoto University, 53 Kawahara-cho, Shogoin, Sakyo-ku, Kyoto 606-8507, Japan*
[2]*JST, CREST, 4-1-8 Hon-cho, Kawaguchi-shi, Saitama 332-0012, Japan*
[3]*Department of Reproductive Biology, National Research Institute for Child Health and Development, 2-10-1 Ookura, Setagaya-ku, Tokyo 157-8535, Japan*
[4]*Department of Developmental Biology, National Research Institute for Child Health and Development, 2-10-1 Ookura, Setagaya-ku, Tokyo 157-8535, Japan*
[5]*Center for iPS Cell Research and Application (CiRA), Institute for Integrated Cell-Material Sciences, Kyoto University, 53 Kawaharacho, Shogoin, Sakyo-ku, Kyoto 606-8507, Japan*

Practical clinical applications for current induced pluripotent stem cell (iPSC) technologies are hindered by very low generation efficiencies. Here, we demonstrate that newborn human (h) and mouse (m) extra-embryonic amnion (AM) and yolk-sac (YS) cells, in which endogenous *KLF4/Klf4*, *c-MYC/c-Myc* and *RONIN/Ronin* are expressed, can be reprogrammed to hiPSCs and miPSCs with efficiencies for AM cells of 0.02% and 0.1%, respectively. Both hiPSC and miPSCs are indistinguishable from embryonic stem cells in colony morphology, expression of pluripotency markers, global gene expression profile, DNA methylation status of *OCT4* and *NANOG*, teratoma formation and, in the case of miPSCs, generation of germline transmissible chimeric mice. As copious amounts of human AM cells can be collected without invasion, and stored long term by conventional means without requirement for in vitro culture, they represent an ideal source for cell banking and subsequent 'on demand' generation of hiPSCs for personal regenerative and pharmaceutical applications.

Introduction

Induced pluripotent stem cells (iPSCs) have been generated through nuclear reprogramming of somatic cells via retrovirus or lentivirus-mediated transduction of exogenous reprogramming factors Oct4, Sox2, Klf4 and C-Myc (Yamanaka 2007). This has led to greatly enhanced promise for exploring the causes of, and potential cures for, many genetic diseases, as well as increased promise for regenerative medicine. Improvements in delivery methodology have further facilitated iPSC generation by minimizing the requirement for genetic modification (Feng *et al.* 2009). Notably, generation of genetic modification-free iPSCs with reprogramming proteins (Kim *et al.* 2009; Zhou *et al.* 2009) suggests regenerative medicine with personal iPSCs could soon be realized. However, the markedly low efficiency of iPSC generation, with all adult somatic cell types tested to date, remains problematic (Wernig *et al.* 2008). Technological advancements in this field have mainly been achieved using mouse embryonic fibroblasts (MEFs), in which the efficiency of iPSC generation is 10–100 times higher than that with adult somatic cells (Yu *et al.* 2007; Wernig *et al.* 2008). Therefore, current methods would appear to be less than ideal for generating iPSCs from adult somatic cells.

Communicated by: Fuyuki Ishikawa
**Correspondence*: ttada@frontier.kyoto-u.ac.jp

DOI: 10.1111/j.1365-2443.2009.01356.x

Here, to find nuclear reprogramming-sensitive cells collectable with no risk by physical invasion, we generated iPSCs from human and mouse newborn extra-embryonic membranes, amnion (AM) and yolk sac (YS), which consist huge amounts of discarded cells after birth. Interestingly, the efficiency of mouse iPSC (miPSC) generation from the AM was comparable to that of MEFs by retroviral transduction with *Oct4*, *Sox2*, *Klf4* and *c-Myc*. Importantly, human iPSC (hiPSC) is also efficiently generated from human AM cells. Expression of the endogenous *KLF4/Klf4*, *c-MYC/c-Myc* and *RONIN/Ronin* in human/mouse AM cells may function in facilitating the generation efficiency of iPSCs. The human AM cell, which is conventionally freeze-storable, could be a useful cell source for the generation of pluripotent stem cells including iPSCs mediated by nuclear reprogramming in the purpose of personal regenerative and pharmaceutical cure in the future of infants.

Results

Generation of iPSCs from mouse AM and YS cells

Extra-embryonic membranes, AM (amniotic ectoderm and mesoderm layers) and YS (visceral yolk sac endoderm and mesoderm layers) express a high level of proto-oncogene (Curran *et al.* 1984) which function, at least in part, to maintain and protect the fetus in utero. In E18.5 mouse embryos just before birth, AM and YS can be easily recognized microscopically (Fig. 1a). The membranes were dissected from *Oct4-GFP* (OG)/*Neo-LacZ* (Rosa26) embryos as approximately 5–10 mm^2 sections and digested with collagenase. Isolated cells were cultured for 4–5 days resulting in morphologically heterogeneous populations (Fig. 1a) in which OG expression was undetectable. Approximately 1×10^5 cells were then retrovirally transfected with exogenous Oct4, Sox2, Klf4 and c-Myc (OSKM). After approximately 3 weeks, OG-positive embryonic stem cell (ESC)-like miPSC colonies were picked and expanded without drug selection. All AM (female) and YS (male)-miPSC lines generated here, which closely resembled ESCs in morphology (Fig. 1a), had a $2n = 40$ normal karyotype (data not shown).

Characterization of AM and YS-miPSCs

As with ESCs, all AM- and YS-miPSC colonies were positive for alkaline phosphatase (ALP) (Fig. 1b). Immunohistochemical analyses also demonstrated that the cells were positive for pluripotent cell-specific nuclear proteins Oct4 and Nanog, and the surface glycoprotein SSEA1 (Fig. 1b). Thus, the expression profile of all marker proteins tested in AM and YS-miPSCs was similar to that observed in ESCs.

To examine the global transcription profile of these cells, comparative Affymetrix gene expression microarray analyses were performed between AM cells, YS cells, YS-miPSCs and R1 ESCs (Fig 1c). The global gene expression profile of YS-miPSCs was significantly different from that of YS cells. We detected a similar behavior between AM-miPSCs and AM cells (data not shown). Notably, the profile was similar to that of ESCs (Fig. 1c). Together, the data indicate that significant global nuclear reprogramming had occurred in these cells in response to OSKM transfection. We next applied RT-PCR analysis to gain a more focused transcriptional profile of pluripotent cell-specific marker genes in the induced cells. We found that *Nanog*, *Rex1*, *ERas*, *Gdf3*, *Zfp296* and *Ronin* were expressed in both AM and YS-miPSCs, whereas the AM and YS genes, *Igf1* and *Ccl6* were silenced (Fig. 1c). Notably, *Ronin* was expressed not only in AM and YS-miPSCs but also in the precursor AM and YS cells. To investigate whether the exogenous *Oct4*, *Sox2*, *Klf4* and *c-Myc* genes were silenced by DNA methylation as reported for other iPSCs (Jaenisch & Young 2008) in the AM and YS-miPSCs, we examined expression using gene-specific primer sets designed to distinguish endogenous and exogenous transcripts. In all miPSC lines, the expression of endogenous *Oct4*, *Sox2*, *Klf4* and *c-Myc* was similar to that in R1 ESCs, whereas the exogenous *c-Myc* and *Klf4* were fully silenced in some YS-miPSC clones but not in others (Fig. 1c). Notably, high-level expression of endogenous *Klf4* and *c-Myc* was detected even in AM and YS cells, consistent with the expression of proto-oncogene (Curran *et al.* 1984). Endogenous expression of *Klf4*, *c-Myc* and *Ronin* genes that are involved in maintaining pluripotency may play a key function in enhancing the generation efficiency of miPSCs from AM and YS cells.

Timing and efficiency of miPSC generation

The molecular mechanisms that govern OKSM-induced nuclear reprogramming of somatic cells to iPSCs are poorly understood. It has been demonstrated that activation of endogenous *Oct4* may be a landmark for irreversible epigenetic transition toward

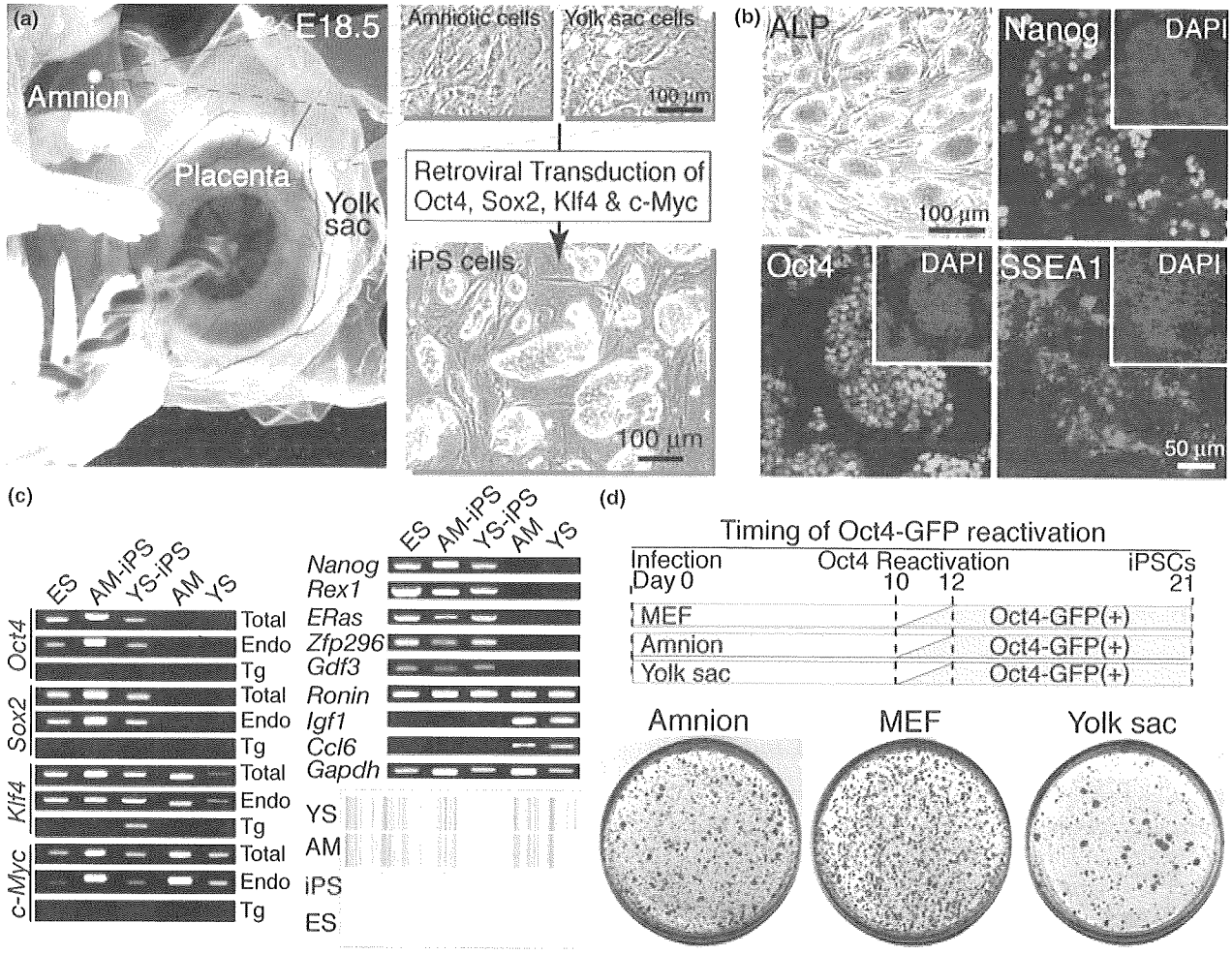

Figure 1 Generation of iPSCs from mouse AM and YS cells. (a) Isolation of AM and YS cells from the extra-embryonic tissues of newborn mice and generation of miPSCs through epigenetic reprogramming by retroviral infection-mediated expression of *Oct4*, *Sox2*, *Klf4* and *c-Myc*. (b) Expression of pluripotent cell marker proteins, alkaline phosphatase (ALP), Nanog, Oct4 and SSEA1. Cell nuclei were visualized with DAPI. (c) Transcriptional activation and silencing of pluripotent and somatic cell marker genes by miPSC induction. RT-PCR analyses revealed that pluripotent marker genes were activated, somatic marker genes were silenced, and *Klf4*, *c-Myc* and *Ronin* were expressed even in AM and YS cells. *Gapdh* is a positive control. Microarray analyses demonstrated global alteration in gene expression profile between YS cells and YS-miPSCs, which more closely resemble mESCs. Relative level of gene expression is illustrated as red > yellow > green. (d) The generation efficiency of ALP-positive colonies and timing of GFP detection demonstrating *Oct4-GFP* reporter gene reactivation. ALP-positive colonies (red) in a 10-cm culture dish was shown when 1.0×10^5 of AM cells, YS cells and MEFs were exposed to OSKM reprogramming factors and reseeded at day 4.

fully reprogrammed iPSCs (Sridharan & Plath 2008). Thus, the timing of reactivation of OG is closely linked with the efficiency of reprogramming. Activation of exogenous OG was detected in some cell populations in every colony around 10 days after OSKM transfection of AM and YS cells, similar to control MEFs examined here and those reported previously (Fig. 1d) (Brambrink *et al.* 2008). The reprogramming efficiency of AM and YS cells was estimated by ALP-staining 21 days after OSKM transfection with reseeding at day 4. Notably, the number of ALP-positive colonies was similar between AM cells (4373 ± 983; mean ± SEM, $n = 3$) and MEFs (4997 ± 1049, $n = 3$), and ~50% in YS cells (2293 ± 487, $n = 3$). Thus, the efficiency of AM reprogramming by OSKM is comparable to that of MEFs, and far exceeds that of adult somatic cells (Fig. 1d).

Germline-transmissible chimeras with AM and YS-miPSCs

To address *in vivo* differentiation potential of the AM and YS-miPSCs, approximately 10 agouti miPSCs were microinjected into C57BL/6J × BDF1 blastocysts (black), and transferred into white ICR foster mothers to generate chimeras. Three male YS-miPSC and two female AM-miPSC lines were tested for chimera formation. X-gal staining analysis on sections of E15.5 embryos demonstrated successful generation of normally developing chimeric embryos with OG/*Neo-LacZ* miPSC contribution to the majority of tissues in all miPSC lines examined (data not shown). We next examined the miPSC potential for normal growth to sexual maturity and germline transmission. Two high-degree chimeric mice with a YS-miPSC line and three high-degree chimeric mice with two AM-miPSC lines, characterized by the >50% contribution of agouti coat color (Fig. 2a), developed normally into adulthood. However, an adult YS-miPSC chimera developed a neck tumor around 8–10 weeks after birth, which may be due to reactivation of the exogenous *c-Myc* as reported previously (Nakagawa *et al.* 2008). Testes isolated from affected males were bisected and one-half was X-gal-stained for LacZ activity whereas the other half was cryosectioned. Blue staining in the seminiferous tubule indicated that YS-miPSCs could contribute to germ cell development. To confirm this, testis cryosections immunohistochemically stained with antibodies against LacZ (iPSC-derived cell marker) and TRA98 (spermatogonia and spermatocyte marker) (Fig. 2b). Germ cells in all tubules were positive for TRA98, whereas germ cells in only some seminiferous tubules were positive for LacZ, clearly demonstrating that YS-miPSCs are capable of contributing to the differentiating germ line in chimeras. Finally, to examine whether the genetic information of YS-miPSCs was transmissible to the next generation, DNA isolated from progeny of the remaining YS-miPSC chimera was analyzed by genomic PCR with a primer set specific to *Neo*. Seven of the thirty-five pups examined were positive, demonstrating that YS-miPSCs are able to differentiate into fully functional germ cells (Fig. 2c). In one of three female AM-miPSC chimeric mice, competence for contribution to germ cells was detected by X-gal staining analysis of ovaries (data not shown).

Teratoma formation with AM and YS-miPSCs

The differentiation competence of AM and YS-miPSCs was further tested by teratoma formation induced by injection of cells into the inguinal region of immunodeficient SCID mice. Teratomas were isolated 5–8 weeks after for histological analysis and for gene expression analysis. Hematoxylin–eosin (HE) staining of paraffin sections demonstrated that the three primary layers were generated as morphologically shown by ectodermal glia and neuroepithelium, mesodermal muscle and endodermal ciliated epithelium and cartilage (Fig. 2d). Multi-lineage differentiation of miPSCs was verified by transcription of endodermal, mesodermal and ectodermal genes in the majority of teratomas (Fig. 2e).

Generation of iPSCs from human AM cells

To examine whether hiPSCs could be efficiently generated from primary AM cells isolated from the amniotic membrane (~100 cm^2) of the placenta of newborn human (Fig. 3a), the reprogramming factors *OCT4*, *SOX2*, *KLF4* and *c-MYC* were introduced by vesicular stomatitis virus G glycoprotein (VSV-G) retroviral transduction. About 20 AM-hiPSC lines were established from 1.0×10^5 AM cells infected (0.02%). The efficiency of AM-hiPSC generation is markedly high relative to that with cells from human adult tissues (Yu *et al.* 2007). AM-hiPSCs were morphologically similar to human ESCs (hESCs) (Fig. 3a). Immunohistochemical analyses demonstrated expression of the pluripotent cell-specific nuclear proteins OCT4, SOX2 and NANOG, and the keratan sulfate proteoglycan TRA-1-60 (Fig. 3b) consistent with the profile observed in hESCs. To extend this analysis, we examined the expression profile of genes by RT-PCR. The endogenous reprogramming factor genes *OCT4*, *SOX2*, *KLF4* and *c-MYC* were all activated in AM-hiPSCs, whereas the transgenes were fully silenced (Fig. 3c). Expression of pluripotent cell-specific genes *NANOG, REX1, GDF3, ESG1, FGF4, TERT* and *RONIN* were also activated in all AM-hiPSC clones consistent with the profile of control hESCs (Fig. 3c). Notably, transcription of *KLF4, c-MYC,* and *RONIN* was detected not only in AM-hiPSCs but also AM cells. Similar to mouse AM and YS cells, endogenous expression of *KLF4, c-MYC* and *RONIN* in human AM cells may facilitate acquisition of reprogramming competency for efficient generation of hiPSCs.

DNA methylation of OCT4 and NANOG in AM-hiPSCs

To further characterize the pluripotent nature of AM-hiPSCs, the promoter CpG methylation status

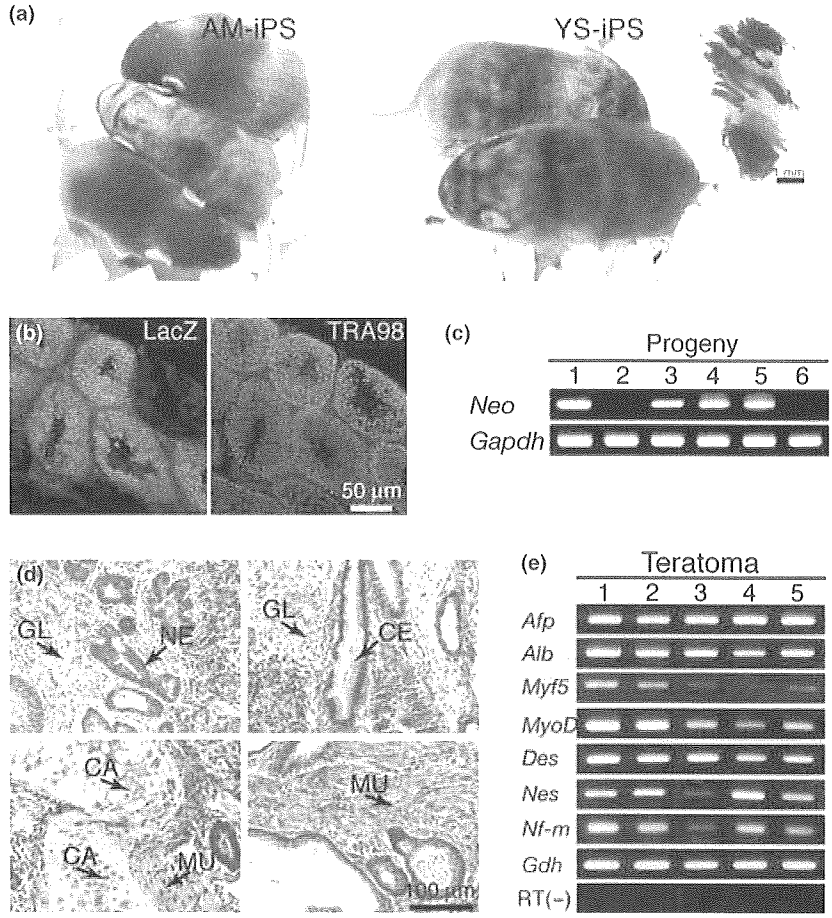

Figure 2 Pluripotency of AM and YS-miPSCs. (a) Chimeric mice with female AM-miPSCs and male YS-miPSCs. Inset: X-gal staining of testis collected from an adult YS-miPSC chimera (blue cells are YS-miPSC derivatives). (b) Immunohistochemical double staining of testis cryosections from a YS-miPSC chimera with anti-LacZ (YS-miPSC-derived germ cells) and anti-TRA98 (spermatogonia and spermatocytes) antibodies. (c) Genotyping of progeny obtained by backcrossing with YS-miPSC chimeras. *Neo* positive demonstrates germline transmission of YS-miPSC genetic information. *Gapdh* is positive control. (d) Hematoxylin-eosin staining of teratoma sections generated by AM and YS-miPSC implantation. GL, glia (ectoderm); NE, neuroepithelium (ectoderm); CE, ciliated epithelium (endoderm); CA, cartilage (ectoderm); MU, muscle (mesoderm). (e) Transcription analysis of lineage-specific genes in teratomas generated with AM and YS-miPSCs. Gray rectangle: endoderm makers; purple rectangle: mesoderm markers; pink rectangle: ectoderm markers. *Afp*, *α-Fetoprotein*; *Alb*, *albumin*; *Des*, *desmin*; *Nes*, *Nestin*; *Nf-m*, *neurofilament-M*; *Gdh*, *Gapdh* (positive control).

of key pluripotency genes was examined by bisulfite-modified DNA sequencing. Promoters of both *OCT4* and *NANOG* were found to highly methylated in hAM cells, consistent with transcriptional silencing in these cells. Conversely, both promoter regions were hypo-methylated in AM-hiPSCs consistent with the observed reactivation (Fig. 3d). These data demonstrate that human AM cells are capable of being epigenetically reprogrammed to AM-hiPSCs through forced expression of reprogramming factors.

Teratoma formation with AM-hiPSCs

To address whether the AM-hiPSCs have competence to differentiate into specific tissues, teratoma formation was induced by implantation under the kidney capsule of immunodeficient nude mice. Twenty-one out of twenty-four AM-hiPS independent clones induced teratoma formation within 6–10 weeks of implantation (1.0×10^7 cells/site). Histological analysis by HE staining of paraffin-embedded sections demonstrated that the three

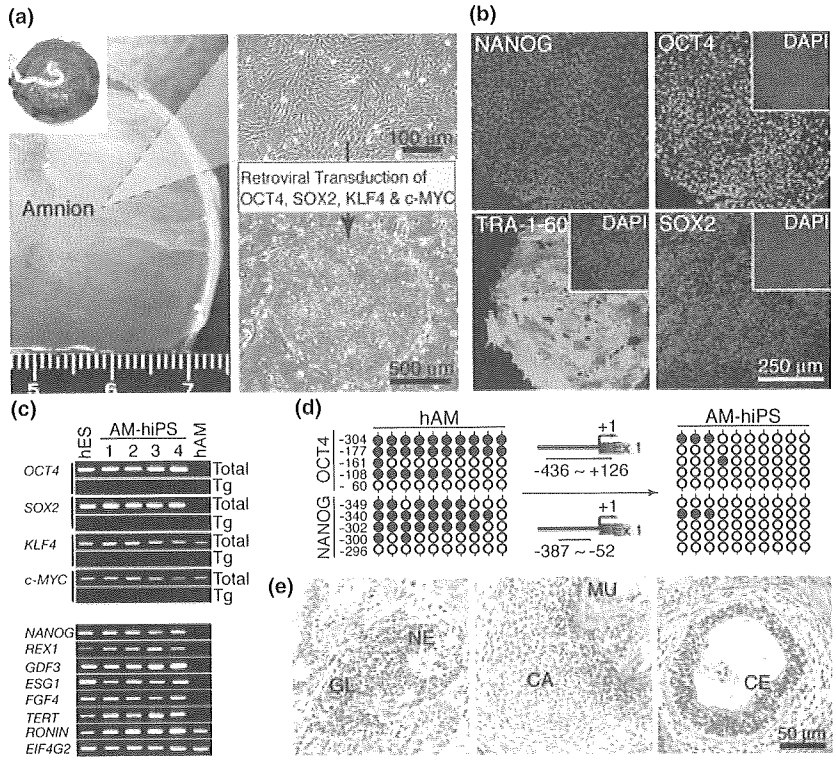

Figure 3 Generation of iPSCs from human AM cells. (a) Isolation of hAM cells from extra-embryonic tissues of human newborns and generation of hiPSCs through epigenetic reprogramming by retroviral infection-mediated expression of *OCT4*, *SOX2*, *KLF4* and *c-MYC*. (b) Expression of pluripotent cell marker proteins, NANOG, OCT4, TRA-1-60 and SOX2. Cell nuclei were visualized with DAPI. (c) Transcriptional activation of pluripotent marker genes by hiPSC induction. RT-PCR analyses revealed that the exogenous *OCT4*, *SOX2*, *KLF4* and *c-MYC* genes were silenced and the endogenous pluripotent marker genes were activated in AM-hiPSCs. *KLF4*, *c-MYC* and *RONIN* were expressed even in hAM cells before reprogramming. *EIF4G2* (*eukaryotic translation initiation factor 4 gamma 2*) is included as a positive control. (d) Epigenetic reprogramming of the *OCT4* and *NANOG* promoter regions. Bisulfite-modified DNA sequence analysis demonstrated a transition from hyper-methylation in AM cells (black circles) to hypo-methylation in AM-hiPSCs (white circles). (e) Hematoxylin-eosin staining of teratoma sections of teratoma generated by AM-hiPSC implantation. GL, glia (ectoderm); NE, neuroepithelium (ectoderm); CE, ciliated epithelium (endoderm); CA, cartilage (ectoderm); MU, muscle (mesoderm).

primary layers were generated as shown by ectodermal glia and neuroepithelium, mesodermal muscle and endodermal ciliated epithelium and cartilage morphologically (Fig. 3e). Thus, the majority of AM-hiPSC clones have potential for multi-lineage differentiation *in vivo*.

Discussion

We here demonstrated that hiPSCs and miPSCs were efficiently generated from newborn AM cells, in which endogenous *Klf4*, *c-Myc* and *Ronin* were highly expressed. The generation efficiency of miPSCs from AM cells was comparable to that from MEFs in mice and was notably high to that from adult somatic cells in humans. The properties of AM-hiPSCs and AM or YS-miPSCs resemble those of fully reprogrammed iPSCs from other tissues and ESCs.

iPSCs are generated through epigenetic reprogramming of somatic cells. Information on the base sequence of DNA in nuclei is unchanged through the reprogramming, although the gene expression profile is altered through the reprogramming from the somatic cell to the iPSC type. Developmentally rewound iPSCs retain aged DNA base sequence information inherited from somatic cells. The base sequence of DNA accumulates mutations through aging with cell division and mis-repair. Young somatic cells are suitable for iPSC generation rather than aged somatic cells. Therefore, it is suggested that the AM cells accumulating less genetic mutation are safer than the adult somatic cells as a cell source for iPSC generation.